1 **Responses of field-grown maize to different soil types, water regimes, and**

2 **contrasting vapor pressure deficit**

3 Thuy Huu Nguyen[1], Thomas Gaiser[1], Jan Vanderborght[3], Andrea Schnepf[3], Felix Bauer[3], Anja

4 Klotzsche[3], Lena Lärm[3], Hubert Hüging[1], Frank Ewert[1, 2]

5 [1]University of Bonn, Institute of Crop Science and Resource Conservation (INRES), Katzenburgweg 5, 53115

6 Bonn, Germany

7 [2]Leibniz Centre for Agricultural Landscape Research (ZALF), Institute of Landscape Systems Analysis,

8 Eberswalder Strasse 84, 15374 Muencheberg, Germany

9 [3]Agrosphere (IBG-3), Institute of Bio- and Geosciences, Forschungszentrum Jülich GmbH, 52428, Jülich,

10 Germany

11 [*]Corresponding author, email: tngu@uni-bonn.de

12 **Abstracts**

13 Drought is a serious constraint to crop growth and production of important staple crops such as maize.

14 Improved understanding of the responses of crops to drought can be incorporated into cropping system

15 models to support crop breeding, varietal selection and management decisions for minimizing negative

16 impacts. We investigate the impacts of different soil types (stony and silty) and water regimes (irrigated

17 and rainfed) on hydraulic linkages between soil and plant, as well as root: shoot growth characteristics.

18 Our analysis is based on a comprehensive dataset measured along the soil-plant-atmosphere pathway at

19 field scale in two growing seasons (2017, 2018) with contrasting climatic conditions (low and high VPD).

20 Roots were observed mostly in the topsoil (10-20 cm) of the stony soil while more roots were found in the

21 subsoil (60-80 cm) of the silty soil. The difference in root length was pronounced at silking and harvest

22 between the soil types. Total root length was 2.5 - 6 times higher in the silty soil compared to the stony

23 soil with the same water treatment. At silking time, the ratios of root length to shoot biomass in the rainfed

24 plot of the silty soil (F2P2) were 3 times higher than those in the irrigated silty soil (F2P3) while the ratio

25 was similar for two water treatments in the stony soil. With the same water treatment, the ratios of root

26 length to shoot biomass of silty soil was higher than stony soil. The seasonally observed minimum leaf

27 water potential (ψ_{leaf}) varied from around -1.5 MPa in the rainfed plot in 2017 to around -2.5 MPa in the

28 same plot of the stony soil in 2018. In the rainfed plot, the mimimum ψ_{leaf} in the stony soil was lower than

29 in silty soil from -2 to -1.5 MPa in 2017, respectively while these were from -2.5 to -2 MPa in 2018,

30 respectively. Leaf water potential, water potential gradients from soil to plant roots, plant hydraulic

31 conductance (K_{soil_plant}), stomatal conductance, transpiration, and photosynthesis were considerably

32 modulated by the soil water content and the conductivity of the rhizosphere. When the stony soil and silt

33 soil are compared, the higher 'stress' due to the lower water availability in the stony soil resulted in less

34 roots with a higher root tissue conductance in the soil with more stress. When comparing the rainfed with

35 the irrigated plot in the silty soil, the higher stress in the rainfed soil resulted in more roots with a lower

36 root tissue conductance in the treatment with more stress. This illustrates that the 'response' to stress can

37 be completely opposite depending on conditions or treatments that lead to the differences in stress that

38 are compared. To respond to water deficit, maize had higher water uptake rate per unit root length and

39 higher root segment conductance in the stony soil than in the silty soil, while the crop reduced transpired

40 water via reduced aboveground plant size. Future improvements of soil-crop models in simulating gas

41 exchange and crop growth should further emphasize the role of soil textures on stomatal function,

42 dynamic root growth, and plant hydraulic system together with aboveground leaf area adjustments.

43 **Key words:** irrigation, plant hydraulic conductance, transpiration, root length, soil types, soil to leaf water

44 potential, stomatal regulation

45 **Abbreviations:** DOY: day of the year; DAS: day after sowing; TUE: transpiration use efficiency; SF: sap flow;

46 LAI: green leaf area index; PAR: photosynthetically active radiation; VPD: vapor pressure deficit; An: net

47 leaf photosynthesis; E: leaf transpiration; ψ_{leaf}: leaf water potential; $\psi_{sunlitleaf}$: leaf water potential of sunlit

48 leaf; $\psi_{shadedleaf}$: leaf water potential of shaded leaf; K_{soil}: hydraulic conductance of soil; K_{root}: root hydraulic

49 conductance; K_{stem}: stem hydraulic conductance; ψ_{soil_effec}: effective soil water potential; $\psi_{difference}$:

50 difference between effective soil water potential and sunlit leaf water potential; K_{soil_root}: root system

51 hydraulic conductance (includes soil and root hydraulic conductance); K_{soil_plant}: whole plant hydraulic

52 conductance (includes below and aboveground components).

53 **1. Introduction**

54 Maize (*Zea mays L.*) is a major staple crop throughout the world. Drought stress, which negatively affects

55 crop growth and yield, is of increasing concern in several important maize cultivating regions (Daryanto et

56 al., 2016). Increases in frequency and severity of drought events due to climate change have been recently

57 reported (IPCC, 2022). Thus, field observations and understanding on how maize responds to water stress

58 are necessary to suggest promising traits for breeding programs (Vadez et al., 2021) as well as irrigation

59 schemes (Fang and Su, 2019; Q. Cai et al., 2017). Improved understanding of crops' response to drought

60 can be incorporated into soil-crop models (e.g. crop modelling and soil-vegetation-atmosphere transfer

61 modelling).

62 Stomatal regulation is often considered as a key aboveground hydraulic variable in regulating water use

63 of crops. Maize ~~was~~ is considered as isohydric plant in which stomata are closed in response to sensing

64 drought conditions to maintain leaf water potential (ψ_{leaf}) above critical levels ($\psi_{threshold}$ or minimum ψ_{leaf})

65 (Tardieu and Simonneau, 1998). ~~Investigations of how stomatal controls differ among species and~~

66 ~~genotypes commonly observed minimum ψ_{leaf} or analyzed of genetic variability of stomatal control in~~

67 ~~response to varying soil water content. Analyzing measurements of ψ_{leaf} from 400 lines of maize of tropical~~

68 ~~and European origins under greenhouse and growth chamber conditions, Welcker et al. (2011) reported~~

69 ~~values of minimum ψ_{leaf} from -0.8 to -1.5 MPa, indicating genetic variability of stomatal responses.~~ The

70 isohydric behavior is due to different mechanisms including hydraulic and/or chemical (e.g. abscisic acid

71 [ABA]) signals (Tardieu, 2016). The degree to which these underlying mechanisms interact and differ

72 among genotypes and/or environmental scenarios in explaining the stomatal regulation is still debated

73 (Tardieu, 2016;, Hochberg et al., 2018). Field evidence in variation of the minimum ψ_{leaf} of maize due to

74 soil water availability and soil hydraulics is rarely reported.

75 Water flow along the soil-plant-atmosphere continuum is determined by a series of hydraulic

76 conductivities and gradients in water potential. Hydraulic conductance of soil (K_{soil}), root hydraulic

77 conductance (K_{root}), and stem hydraulic conductance (K_{stem}) determine water potential from soil to root

78 and root xylem water, and thus magnitude of ψ_{leaf}. There are two main resistances to water flow from the

79 soil to the shoot, namely the soil and the root resistances, often expressed as their inverse, K_{soil} and K_{root}

80 (Nguyen et al., 2020; Cai et al., 2018). In wet soils, the soil hydraulic conductivity is much higher than that

81 of roots, and water flow is mainly controlled by root hydraulic conductivity (Hopmans and Bristow, 2002;

82 Draye et al., 2010). It is well-known that a decrease in soil matric potential and soil hydraulic conductivity

83 triggers stomatal closure and thus results in reduction in transpiration rate (Sinclair and Ludlow, 1986;

84 Carminati and Javaux 2020; Abdalla et al., 2021). For the root water uptake and controlling stomata, the

85 location where soil and roots are in close contact (rhizosphere) is most important, because when this thin

86 layer of rhizosphere is disconnected (i.e. soil-root contact is lost), the water movement from soil toward

87 the roots is reduced, which might trigger stomatal closure to maintain hydraulic integrity of plant

88 (Carminati et al., 2016; Rodriguez-Dominguez and Brodribb, 2019; Abdalla et al., 2022). The magnitude of

89 the drop of water potential between bulk soil and soil-root interface increases considerably at different

90 levels of soil dryness for different soil types (Carminati and Javaux, 2020; Abdalla et al., 2022). Hydraulic

91 limits in the soil (Carminati and Javaux, 2020), or in the root–soil interface [as measured for olive trees by

92 Rodriguez-Dominguez and Brodribb, 2019 or tomato (Abdalla et al., 2022)], or in the root properties

93 (Bourbia et al., 2021; Cai et al., 2022; Nguyen et al., 2020; Cai et al., 2018) or due to both soil textures and

94 root phenotypes (Cai et al., 2022b) emphasized the importance of belowground hydraulics (Carminati and

95 Javaux, 2020). However, also the shoot hydraulic conductance could be limiting in some crop plants

96 (Gallardo et al., 1996) or in trees (Domec and Pruyn, 2008; Tsuda and Tyree, 1997). Stomatal conductance

97 and shoot hydraulic conductance showed close links to each other in pine trees (Hubbard et al., 2001).

98 This summary illustrates three points: (i) current studies have often focused either on above or on below

99 hydraulic limits, but rarely consider both (ii) it is unclear the roles and relations of soil hydraulic properties

100 to root and plant hydraulic conductance (thus influences on stomatal conductance) (iii) the role of different

101 hydraulic processes across the soil - plant - atmosphere continuum i.e. soil to roots, stem, and soil-plant

102 hydraulic conductance in controlling stomatal conductance remains unclear.

103 Simultaneous measurements of atmospheric conditions (light intensity and vapor pressure deficit), leaf

104 water potential, and transpiration rates, coupled with measurements of root, stem and whole soil-plant

105 hydraulic conductance, root architecture, and soil water potential distribution could reveal the relative

106 importance of rhizosphere, shoot and root growth, and hydraulic conductance vulnerability, especially

107 under progressive soil drying at field conditions (Carminati and Javaux, 2020; Tardieu et al., 2017). For the

108 soil water conditions, soil texture and hydraulic characteristics are very important ~~that~~ because they

109 influence soil water movement and thus affect infiltration, surface and sub-surface runoff, and ultimately

110 plant available soil water (Vereecken et al., 2016). Soil texture properties, characterized by different

111 fractions of clay, silt, and sand particles, are important drivers in determining the soil water retention

112 properties (Scharwies and Dinneny, 2019; Stadler et al., 2015; Zhuang et al., 2001). Soil with higher water

113 holding capacity (here the silty soil with low stone content) have a larger amount of plant available water

114 which in turn enables crops to better meet the evaporative demand and facilitates better crop growth as

115 compared to the soil with high stone content (Nguyen et al., 2020; Cai et al., 2018). Estimations of hydraulic

116 conductance (different organs and whole plant hydraulic conductance) were done for crop plants and

117 maize mainly under controlled environment or pot conditions e.g. for different species and genotypes

118 during soil drying (Sunita et al., 2014; Choudhary and Sinclair, 2014; Abdalla et al., 2022; Meunier et al.,

119 2018; Wang et al., 2017; Li et al., 2016) or various species and genotypes together with different soil

120 textures (Cai et al., 2022a), or soil texture with different vapor pressure deficit (VPD) (Cai et al., 2022b).

121 Compared to the substantial effect of soil texture, there was no evidence of an effect of VPD on both soil–

122 plant hydraulic conductance and on the relation between canopy stomatal conductance and soil–plant

123 hydraulic conductance in pot-grown maize (Cai et al., 2022b). Contrast results were found in winter wheat

124 where plant hydraulic conductance increased with rising VPD for some genotypes in wet conditions

125 (Ranawana et al., 2021). Vadez et al., (2021) examined the effects of soil types together with increasing

126 VPD on transpiration efficiency (TE) and yield under pot conditions for several C_4 species (maize, sorghum,

127 and millet). The interpretation of differences in TE was attributed to soil types, more specifically, to the

128 differences in soil hydraulic properties and soil hydraulic conductance. However, experimental evidence

129 linking root hydraulics to stomatal regulation was lacking in these two Vadez's studies (Vadez et al., 2021).

130 ~~Extrapolation and use of results obtained in pots or under greenhouse conditions to the field scale are~~

131 ~~difficult due to the fact that soil substrates in pots might not represent natural soil in the field (Passioura,~~

132 ~~2006). There is often greater evaporative demand and considerable fluctuation and interactions of climatic~~

133 ~~variables in the field as compared to experiments under controlled or semi-controlled conditions.~~ Recent

134 field studies have aimed at quantification of root hydraulic conductance and it's linkages with crop growth

135 (leaf area and biomass) under different soil types (in wheat Cai et al., 2017; Cai et al., 2018; Nguyen et al.,

136 2020 or maize in Nguyen et al., 2022; Jorda et al., 2022). However, field studies that consider both below

137 (soil-root hydraulic conductance) and above (stem hydraulic conductance), or soil-plant hydraulic

138 conductance (including below and above-ground parts) and their roles in stomatal regulation as well as

139 crop growth (leaf area and biomass) are rarely carried out.

140 This study aims at further understanding of the hydraulic linkages between soil and plant and responses

141 of plants to drought stress in relation to root: shoot growth characteristics at field scale. We hypothesize

142 that, in field-grown maize, (1) soil-plant hydraulic conductance depends on soil hydraulic properties,

143 especially under dry soil conditions (2) minimum leaf water potential of maize is similar across soil types,

144 water treatments and climatic conditions. The hypotheses will be tested through three objectives: (i) to

145 investigate the effects of soil types, water application, and climatic condition on root growth and (ii) on

146 stomatal conductance, leaf photosynthesis, transpiration, leaf water potential, different components

147 ~~(root, stem and whole soil-plant~~ of ~~the~~ hydraulic conductance (root, stem, and whole soil-plant), and (iii)

148 to analyze the relative contribution of root and shoot growth (leaf area and biomass) on the water uptake

149 capacity of maize. These three objectives will be achieved based on a comprehensive dataset covering the

150 whole soil-plant continuum over two growing maize seasons with contrasting climatic conditions (low and

151 high VPD) under two water treatments (rainfed and irrigated) and two different soil types (stony and silty

152 soil).

153 **2. Materials and methods**

154 **2.1. Location and experimental set-up**

155 We carried out a field experiment at two rhizotron facilities in Selhausen, North Rhine-Westphalia,

156 Germany (50°52'N, 6°27'E). The field is slightly inclined with a maximum slope of around 4°. One rhizotrone

157 facility was located upslope (F1) with around 60% gravel by weight in the 10-cm topsoil while the second

158 rhizotrone facility was at downslope (F2) with silty soil (stone content is around 4% by weight).

159 Each ~~experimental site~~rhizotrone facility was divided into three subplots of 7.25 m by 3.25 m: two rainfed

160 plots (P1, P2), and one irrigated plot (P3). In rainfed plots P1, other sowing densities and dates were used

161 than in the other plots and we excluded therefore these plots. Silage maize *cv.* Zoey was sown on 4 May

162 and 8 May in 2017 and 2018, respectively, with a plant density of 10.66 seeds m^{-2} (Figure 1a; Table 1).

163 Detailed information of crop management practices is provided in Table 1.

164 [Insert Table 1 here]

165 **2.2. Water applications**

166 Weather variables (global radiation, temperature, relative humidity, precipitation, and wind speed) were

167 recorded every 10 minutes by a nearby weather station (approx. 100 m from the experiment). Drip lines

168 (T-Tape 520-20-500, Wurzelwasser GbR, Müzenberg, Germany) were installed for irrigation at 0.3 m

169 intervals parallel to the crop rows. In 2017, maize received a total amount of 230 mm precipitation during

170 the growing period (136 days). Average, minimum and maximum daily air temperature were 17.6, 8.3, and

171 25.3 °C, respectively (Fig. 1b). The crop on P3 was irrigated (in total 130 mm) every 5-7 days (in total 10

172 times) using 13 mm of irrigation water per event between mid June to end of August for the irrigated plots

173 (2017F1P3 and 2017F2P3) (Fig. 1b). In 2018, average, minimum, and maximum daily air temperature were

174 19.2, 10.85, and 27.3 °C, respectively (Fig. 1b) and exceeded those of 2017. Characterized by exceptionally

175 hot and dry weather conditions, the summer season 2018 can be classified as an extreme year with respect

176 to plant growth at our experimental location~~site~~. Maize experienced high temperatures and VPD,

177 especially around tasseling and silking. In 2018, only 91.3 mm of rain were recorded in the growing period

178 of 2018 (107 days). The maize crop was irrigated every 5-7 days (in total 13 times), with a total amount of

179 irrigation of 257 mm and 239 mm between mid- June and mid- August for the irrigated plots 2018F1P3

180 and ~~2018F1P3~~2018F2P3, respectively (Fig. 1d). In contrast to 2017, the rainfed plot in the stony soil

181 (2018F1P2) had to be irrigated (in total 66 mm) ~~in~~ four times (using 13, 22, 13, and 18 mm, respectively)

182 to avoid a crop failure due to severe drought (Fig. 1d). Detailed estimates of irrigation amount and

183 intervals could be found in Nguyen et al., (2022a).

184 [Insert Figure 1 here]

185 **2.3. Measurements**

186   **2.3.1. Soil water measurement and root growth**

187   At soil depths of 10, 20, 40, 60, 80, and 120 cm, MPS-2 matrix water potential and temperature sensors

188   (Decagon Devices Inc., UMS GmbH München, Germany) were installed to measure half-hourly soil water

189   potential and soil temperature. The range of the water potential measurements is ~~form~~ from -9 kPa to

190   approximately -100000 kPa (pF 1.96 to pF 6.01). In addition to MPS-2, soil water potential was measured

191   by pressure transducer tensiometers (T4e, UMS GmbH, München, Germany) where the minimum

192   detectable suction is -85 kPa to +100 kPa. A detailed description of sensor installation, calibration and data

193   post processing can be found in Cai et al., (2016).

194   Minirhizotubes (7 m long clear acrylic glass tubes with outer and inner diameters of 6.4 and 5.6 cm,

195   respectively) were installed horizontally at six different depths of 10, 20, 40, 60, 80, and 120 cm below the

196   soil surface in each facility. There are three replicate tubes at each depth, accounting for 54 tubes in each

197   facility. Root measurements were taken manually by Bartz camera (Bartz Technology Corporation) (23

198   June 2017 – 12 September2017) and VSI camera (Vienna Scientific Instruments GmbH) (08 June 2017 – 22

199   June 2017) in 2017 while only VSI was used in 2018 (23 May2018 - 23 August 2018). Root images were

200   taken at 20 fixed positions from the left- and right-hand sides of each tube weekly (or biweekly) during the

201   growing seasons~~Root images were repeatedly taken from both left and right sides at 20 locations along~~

202   ~~horizontally installed minirhizotubes~~. The root images were analyzed by automated minirhizotube image

203   analysis pipeline for segmentation and automated feature extraction (Bauer et al., 2021). Two-dimensional

204   root length density (RLD, in units of cm cm^{-2}) was estimated from the total root length observed in the

205   image and the image surface area. The overview of camera system, minirhizotube images acquisition, and

206   post-processing of the root data were described in detail in Bauer et al. (2021) and Lärm et al., (2023).

207   **2.3.2. Crop growth, leaf gas exchange, leaf water potential, and sap flow measurements**

208   ~~**measurement**~~

209   The phenology, plant height, stem diameter, green and brown leaf area, dry matter of different organs,

210   and total aboveground dry matter were observed and measured bi-weekly. Dates of sowing, emerge,

211   tasseling, and silking for two growing seasons were observed. There was difference in emerge, tasseling

212   and silking dates for two growing seasons due to the differences of sowing dates and temperature.

213   However, the developmental stages were not different among water treatments and soil types within one

214   season. Measurements of green leaf area and aboveground dry matter were based on the destructive

215   method. Plant height was measured of 15 randomly selected plants. The diameters of five randomly

216   selected stems were measured. Due to the limited number of plants in each plot, only two plants per

217   measurement date were sampled to determine total aboveground dry matter and leaf area (7 and 8 times

218   in 2017 and 2018, respectively). Green and brown leaf area was measured by a LI-3100C (Licor Biosciences,

219   Lincoln, Nebraska, USA). At harvest, five separate replicates (1m^2 each) were harvested. The dry matter of

220   separate organs was determined after drying at 105 °C for 48 hours (Nguyen et al., 2020).

221   **2.3.3. Leaf gas exchange, leaf water potential, and sap flow measurements**

222   Hourly leaf stomatal conductance (Gs), net photosynthesis (An), and leaf transpiration (E) were measured

223   every two weeks under clear sky conditions. Observations from 8 AM to 5 PM on four days and from 10

224   AM to 4 PM on six days were carried out in 2017. In 2018, measurements were carried out on 6 days from

225   8 AM to 7 PM and on 5 days from 10 AM to 4 PM (Nguyen et al., 2022a). The Gs, An, and E of two sunlit

226   leaves (uppermost fully developed leaves) and one shaded leaf of different plants were measured at

227   steady-state using a LICOR 6400 XT device (Licor Biosciences, Lincoln, Nebraska, USA). After leaf gas

228   exchange measurements, leaves were quickly detached using a sharp knife to measure lLeaf water

229   potential (ψ_{leaf}) was measured with a digital pressure chamber (SKPM 140/ (40-50-80), Skye Instrument

230   Ltd, UK) with the working air pressure ranging from 0 to 35 bars. To study the diurnal course of ψ_{leaf} under

231   dry and re-wetted soil conditions, in 2018, measurements were undertaken for three additional days with

232 predawn measurements two days before and one day after irrigation. ~~Further detail of measurement~~

233 ~~dates, range of real time records of PAR, VPD and soil water status could be found in (Nguyen et al., 2022a).~~

234 In 2017 (from 7 July 2017 until harvest) and 2018 (from 28 June 2018 until harvest), 20 sap flow sensors

235 (SGA 13, SGB 16, and SGB 19 types) were installed (one sensor per plant and 5 maize plants per plot) based

236 on stem diameter size. ~~Sensor data, in particular the partitioning of energy, electricity supply, sap flow,~~

237 ~~and the temperature difference between upper and lower thermocouples (dT) of each sensor were~~

238 ~~recorded at 10 minute intervals using a CR1000 data logger and two AM 16/32 multiplexers (Campbell~~

239 ~~Scientific, Logan, Utah).~~ The sap flow in the plant ($g\ h^{-1}$) was ~~monitored~~ estimated directly by the data

240 loggers (Dynamax, 2007) and used as a surrogate for canopy transpiration based on the number of plants

241 per square meter. Further detail of developmental stages, crop growth, leaf gas exchange, leaf water

242 potential, and sap flow measurements ~~measurement dates, range of real time records of PAR, VPD and~~

243 ~~soil water status~~ could be found in ~~(~~Nguyen et al., (2022a) and Nguyen et al., (2020).

244 **2.4. Calculation of total root length, root system conductance, stem, and whole plant hydraulic**

245 **conductance**

246 To estimate the total root length from minirhizotubes, we adopted the option 2 which was described in

247 Cai et al., (2017). Total root length per square meter soil surface area within each soil layer ($m\ m^{-2}$) was

248 computed by multiplying the root length density with the corresponding soil layer thickness. The root

249 length density was determined in each depth by dividing the measured root length per minirhizotron

250 image by the assumed volume the roots would have occupied in absence of the tube, i.e., W * L * tube

251 radius (see Cai et al., 2017).

252 Following Nguyen et al., (2020), the effective soil water potential was calculated based on hourly measured

253 soil water potential (ψ_i) and normalized root length density at six depths (10, 20, 40, 60, 80, and 120 cm)

254 ($NRLD_i$), and soil layer thickness (Δz_i) in the soil profile (Equation 1).

$$\psi_{soil\_effec} = \sum_{i=1}^{N} \psi_i NRLD_i \, \Delta z_i \tag{1}$$

255   We followed Ohm's law analogy by dividing the hourly sap flow by the difference between effective soil

256   water potential and shaded leaf water potential to estimate root system conductance (K_{soil_root} - Equation

257   2), between shaded leaf water potential and sunlit leaf water potential to estimate stem hydraulic

258   conductance (K_{stem} - Equation 3), and between effective soil water potential and sunlit leaf water potential

259   to estimate whole plant hydraulic conductance (K_{soil_plant} - Equation 4).

$$K_{soil\_root} = Sapflow/(\psi_{soil\_effec} - \psi_{shadedleaf}) \tag{2}$$

$$K_{stem} = Sapflow/(\psi_{shadedleaf} - \psi_{sunlitleaf}) \tag{3}$$

$$K_{soil\_plant} = Sapflow/(\psi_{soil\_effec} - \psi_{sunlitleaf}) \tag{4}$$

260   During one measurement day, four values of the K_{soil_root}, K_{stem}, and K_{soil_plant} were obtained from

261   measurements between 11AM and 2 PM. The average and standard deviation of these hourly

262   measurements were calculated for each measurement day in order to present the seasonal dynamics of

263   those variables. To capture the diurnal and seasonal variations of sap flow and sunlit leaf water potential,

264   in addition, we plotted the hourly sap flow and hourly difference of effective soil water potential and sunlit

265   leaf water potential for three measurement days starting from predawn and whole seasons, respectively,

266   to derive the slope which is also K_{soil_plant}.

267   **2.5. Statistical analysis**
268

269   Regression analysis was performed to understand the relationship between the sap flow volume and the

270   difference of effective soil water potential and sunlit leaf water potential as well as the relationship

271   between the total aboveground biomass and cumulated water transpired (sap flow volume). These

272   analyses allow to derive the slope as proxy of K_{soil_plant} and transpiration use efficiency, respectively. Since

273   all measured data have their own measurement errors, the generalized Deming regression was employed.

274 We performed relationships (via correlation coefficient and statistical significant levels) of midday leaf An,

275 Gs, and E with midday K_{stem}, K_{soil_plant}, K_{soil_root}, sunlit leaf potential, ψ_{soil_effec}, and the difference of ψ_{soil_effec}

276 and sunlit leaf water potential ($\psi_{difference}$). All data processing and analysis were conducted using the R

277 statistical software (R Core Team, 2022).

278 **3. Results**

279 **3.1. Root growth under different water treatments, soil types and climatic conditions**

280 Observed root length (cm cm^{-2}) from the minirhizotubes in different soil depths at the first week of June

281 (stem elongation), around silking, and at harvest in two growing seasons are shown in the Figure 2. Root

282 length was similar among water treatments at the start of stem elongation in both years (Fig. 2a & 2d).

283 The difference in root length was pronounced at silking and harvest between the soil types. More root

284 growth was observed in the silty soil compared to the stony soil with the same water treatment (i.e. 2.5 -

285 6 times higher at depth 40 cm). This indicated the strong negative effects of stone content on root

286 development. In the stony soil, root length in the irrigated plot (F1P3) was slightly higher than in the rainfed

287 plot (F1P2). In contrast, the rainfed treatment (F2P2) in the silty soil showed much higher root length,

288 especially from 40 to 120 cm depths as compared to the irrigated plot (F2P3) in both growing seasons.

289 Much lower stone content and deep soil cracks in the silty soil (Morandage et al., 2021) allow root

290 extension to the subsoil, particularly in the rainfed plot F2P2. Root length in the rainfed treatment (F2P2)

291 in 2018, is higher than in 2017 which implies that root further developed to exploit the water in the soil

292 under the rainfed condition to meet the higher evaporative demand.

293 [Insert Figure 2 here]

294 Total root length (m m^{-2}) estimated from minirhizotubes and its ratio to shoot dry matter (m kg^{-1}) at three

295 measured dates (as in Figure 2) are shown in the Figure 3. Total root length was much higher for the silty

296 plots as compared to stony plots. In 2017, the highest total root length was observed in the rainfed plot of

297 the silty soil (F2P2) with approximately 9166 m m^{-2} and 9878 m m^{-2} around silking and harvest, respectively,

298 which was almost two times higher than in the irrigated plot (F2P3). These figures were higher in 2018

299 than 2017 where total root length of F2P2 was 10188 m m^{-2} and 13750 m m^{-2} at silking and harvest time,

300 respectively. For the rainfed stony soil (F1P2), soil water depletion around the beginning of June in 2017

301 (Supplementary material 1a) and from the first two weeks of June to harvest in 2018 (Supplementary

302 material 2a) caused the strong reduction of shoot biomass. In the stony soil, the shoot dry matter of the

303 irrigated plot (F1P3) and the rainfed plot (F1P2) were 1275 and 536 g m^{-2} at silking time (e.g. 19 July 2018

304 – DOY 200, Supplementary material 3a and 3b). However, there was a minor difference between F1P2 and

305 F1P3 in terms of the ratio of root length to shoot dry matter. In the silty soil, a decrease of soil water

306 potential was not pronounced (compared to stony soil) in both years 2017 and 2018 (Supplementary

307 material 1b and 2b). In 2018, shoot biomass in the irrigated stony soil (F1P3) and silt soil (F2P3) were

308 similar (1275 and 1299 g m^{-2}, respectively on 19 July 2018 – DOY 200) while the shoot biomass of the

309 rainfed silty soil (F2P2) was 876 g m^{-2} (Supplementary material 3a & 3b). However, the ratios of root length

310 to shoot biomass in the rainfed plot of the silty soil (F2P2) were 3 and 6 times higher than those in the

311 irrigated silty soil (F2P3) and stony soil (F1P3), respectively (e.g. 18 July, DOY 199). Moreover, total root

312 length was relatively equal among treatments at the start of set elongation (8 June - DOY 159, first week

313 of June) in both years, while this was the opposite for the ratio of root length to shoot dry matter. This

314 firstly illustrated that the finer soil texture without stones and with soil cracks could favor the root growth

315 which indicates strong interactions of root and soil conditions. Secondly, the larger root length and higher

316 atmospheric evaporative demand in 2018 than 2017 indicates also the interaction of root growth and

317 climatic conditions.

318 [Insert Figure 3 here]

319 **3.2. Stomatal conductance, photosynthesis, transpiration, and K$_{soil\_plant}$**

320 **3.2.1. Diurnal course of stomatal conductance, photosynthesis, transpiration, and water potential at leaf**

321 **level**

322 After a long period with high temperatures and no rainfall, soil water reduction in the rainfed plot of the

323 stony soil (F1P2) on 17 July 2018 (Supplementary material 2) resulted in three times lower net

324 photosynthesis (An), stomatal conductance (Gs), transpiration (E) and leaf water potential (ψ_{leaf}) as

325 compared to the remaining treatments (FigSupplementary material 4. 4). This indicates that the soil water

326 content strongly affected the stomatal conductance. Stomatal closure was much pronounced around

327 midday in F1P2 while this was not the case in the F2P2, indicating the soil type strongly affected the

328 stomatal conductance and leaf gas exchange.

329 [Insert Figure 4 here]

330 Leaf gas exchange and leaf water potential in the F1P2 were still much lower than in other plots (Figure

331 54). On 18 July 2018, after application of 22.75 mm of irrigation water (at 4 PM), photosynthesis, stomatal

332 conductance, transpiration and leaf water potential were slightly increased in F1P2. However, these were

333 still smaller than in F2P2 and the two irrigated plots.

334 [Insert Figure 5 4 here]

335 On the next day after irrigation, leaf gas exchange and water potential were considerably increased in the

336 F1P2 (Figure 6Supplementary material 5). Leaf curling was also less pronounced as compared the two

337 previous days. This indicated the recovery of plant after watering. Leaf water potential, photosynthesis,

338 stomatal conductance, and leaf transpiration were almost similar to other plots from predawn throughout

339 the day.

340 [Insert Figure 6 here]

341 **3.2.2. Seasonal course of stomatal conductance, photosynthesis, transpiration, water potential, and**

342 **plant hydraulic conductance at the leaf level**

343 Seasonal stomatal conductance (Gs) and leaf water potential (ψ_{leaf}) are described in Figure 75. The

344 relationship between two variables was rather noisy and non-linear. The leaf water potential showed

distinct patterns among treatments in one growing season. Minimum ψ_{leaf} was maintained at around -1.5

MPa in the irrigated plot in stony soil (F1P3) and two plots in the silty soil (F2P2 and F2P3). Lower minimum

ψ_{leaf} could be observed in the rainfed plot with stony soil (F1P2) but it did not go beyond -2 MPa. Minor

leaf curling was observed only in the second week of June in the F1P2 in 2017. In 2018, the higher

temperature and vapor pressure deficit resulted in lower minimum ψ_{leaf} in all treatments and soil types as

compared to 2017. The minimum ψ_{leaf} was around -2 MPa in F1P3, F2P2, and F2P3 while ψ_{leaf} could drop

below -2 MPa in F1P2 which was due to the severe soil water deficit. The low Gs and ψ_{leaf} associated with

measurement dates when the substantial leaf curling was observed at mid of July to the end of growing

season in F1P2 in 2018 (Supplementary material 3c & 3d and Supplementary material 4̶6c & d).

[Insert Figure 7̶5 here]

The effective soil water potential ($\psi_{soil\_effect\ MD}$), sunlit leaf water potential ($\psi_{sunlitleaf\ MD}$), stomatal

conductance (Gs_{MD}), and whole plant hydraulic conductance ($K_{soil\_plant\ MD}$) at midday at several times during

the growing season are presented in Figures 8̶6 and 9̶7 for 2017 and 2018, respectively. As expected,

there was not much difference in terms of $\psi_{soil\_effecMD}$ among F1P3, F2P2, and F2P3 from 02 August to one

week before harvest in 2017. The lowest $\psi_{soil\_effec\ MD}$ was observed in the F1P2. Leaf water potential

dropped drastically but also $K_{soil\_plant\ MD}$ increased strongly whereas $\psi_{soil\_effec\ MD}$ remained quite similar (e.g.

18 July). This is because sap flow have increased substantially in this day (e.g. from 2.34 mm d^{-1} on 17 July

to 6.97 mm d^{-1} on 18 July for the F1P2). The stomatal conductance decreased a lot in this day which could

be explained that the atmospheric demand increased (e.g. global radiation was 13.6 MJ m^{-2} on 17 July

compared to 23.9 MJ on 18 July while daily VPD was 0.7 kPa and 1.2 kPa, respectively) even more than the

sap flow. Midday sunlit leaf water potential was not distinctively different among treatments with the

lowest $\psi_{sunlitleaf\ MD}$ around -1.6 MPa throughout season. Also, Gs_{MD} was rather similar among plots. The

$K_{soil\_plant\ MD}$ ranged from 0.125 to 0.96 mm h^{-1} MPa^{-1} with a sharp reduction before harvest. In general, the

lowest values of $K_{soil\_plant\ MD}$ were found in F1P2 which was consistent with the smaller overall seasonal

369   K_{soil_plant} (as the slope of linear relationship between sap flow and difference of effective soil water potential

370   and sunlit leaf water potential) (see Supplementary material 57).

371   [Insert Figure 86 here]

372   The $\psi_{soil\_effec\,MD}$ was substantially different in the two soil types and water treatments in 2018 (Figure 9a7a).

373   Both F1P2 and F1P3 showed a gradual drop of $\psi_{soil\_effec\,MD}$ from 15 June until the third week of July then

374   increased after irrigation events on 18 July (Supplementary material 2b). However, $\psi_{soil\_effec\,MD}$ of F1P2 was

375   much lower than F1P3 toward the harvest. The $\psi_{soil\_effec\,MD}$ of F2P2 and F2P3 only decreased progressively

376   from around 10 July till harvest even though there was water supply from the irrigation (Supplementary

377   material 2b). The water applied by irrigation and coming in by rainfall were insufficient to wet up the

378   deeper soil layers which remained dry. The low Gs_{MD} was corresponding to the lowest $\psi_{sunlitleaf\,MD}$ and

379     $K_{soil\_plant\,MD}$ from the F1P2 (Figure 9c7c & 9d7d). The $K_{soil\_plant\,MD}$ from all plots was ranging from 0.12 to 0.91

380   mm h^{-1} MPa^{-1}. There was the drop in $K_{soil\_plant\,MD}$ (i.e. 3 to 9 July or 17-18 July) before irrigation in this plot.

381   However, it increased after the irrigation (i.e. 10 July and 19 July). This suggests that K_{soil_plant} depends

382   strongly on the soil water content and the conductivity of the rhizosphere.

383   [Insert Figure 97 here]

384   **3.2.3. Relationships of stomatal conductance, transpiration, photosynthesis with plant hydraulic**

385   **variables at the plant canopy level**

386   The slope of linear relationship between sap flow and difference of ψ_{soil_effec} and $\psi_{sunlitleaf}$ is shown for three

387   consecutive days (leaf water potential measurements from the predawn) and before and after irrigation

388   applications (17, 18, and 19 July 2018 or DOY 198, 199 and 200, respectively) (Figure 810). On both DOYs

389   dates 198 17 and 18 July and 199, the difference between ψ_{soil_effec} and $\psi_{sunlitleaf}$ was around -1.6 MPa with

390   very low transpiration rates in the treatment F1P2 which was associated with very low plant hydraulic

391   conductance and leaf curling. The whole plant hydraulic conductance was disrupted on these two days

392 (0.06 and 0.16 mm h^{-1} MPa^{-1} for 17 and 18 July~~DOY 198 and 199~~, respectively). Water was supplied on ~~DOY~~

393 18 July~~199~~ at 1 PM for the irrigated plots (F1P3, F2P3) as well as F1P2 at 4 PM (for saving plant from death

394 due to severe drought stress). K$_{soil\_plant}$ was slightly changed (0.43 and 0.57 mm h^{-1} MPa^{-1} for F1P3 on ~~DOY~~

395 ~~199~~ 18 and 19~~and 200~~ July, respectively and 0.5 and 0.58 mm h^{-1} MPa^{-1} for F2P3 on 18 and 19 July~~DOY 199~~

396 ~~and 200~~, respectively). However, the increase of K$_{soil\_plant}$ was substantial in the F1P2 after the irrigation.

397 Soil water replenishment and an increase in the root - soil contact (Fig. ~~9a~~7a) allowed the K$_{soil\_plant}$ to

398 recover overnight to 0.46 mm h^{-1} MPa^{-1}. This resulted in a narrower water potential gradient between root

399 zone and sunlit leaf and in a higher transpiration rate on 19 July~~DOY 200~~.

400 [Insert Figure ~~10~~8 here]

401 Seasonal average of different midday hydraulic conductance components (root system hydraulic

402 conductance - K$_{soil\_root}$, stem hydraulic conductance – K$_{stem}$, and whole plant hydraulic conductance –

403 K$_{soil\_plant}$) are shown in Figure ~~11~~9. In the same year, the K$_{stem}$ was not much different among F1P3, F2P2,

404 and F2P3 plots. The K$_{stem}$ of those plots was slightly higher than in the F1P2 in both years. In general, the

405 K$_{soil\_root}$ was lower than the K$_{stem}$. Overall, the estimated K$_{soil\_plant}$ was around 1/ (1/K$_{soil\_root}$ +1/K$_{stem}$)

406 regardless of soil types, years, and water treatments. The K$_{soil\_root}$ and K$_{soil\_plant}$ in the F1P2 in 2018 was much

407 lower than the remaining plots while the K$_{soil\_root}$ and K$_{soil\_plant}$ ~~was~~ were not much different among plots in

408 2017. Our results indicated that there was an impact of soil hydraulic conductance on K$_{soil\_root}$ and K$_{soil\_plant}$.

409 ~~The K$_{soil\_plant}$ and K$_{soil\_root}$ depend strongly on the soil water content and the soil hydraulic properties. Overall,~~

410 ~~the estimated K$_{soil\_plant}$ was around 1/ (1/K$_{soil\_root}$ +1/K$_{stem}$) regardless of soil types, years, and water~~

411 ~~treatments.~~ Although there is a large difference in total root length between the two soil types (e.g. F1P3

412 versus F2P2 or F2P3 versus F2P2), K$_{soil\_root}$ and K$_{soil\_plant}$ in those two plots were not much different. This

413 could be explained by the fact that K$_{soil\_plant}$ was not only depended on root length but also depended on

414 the variability of root segment hydraulic conductance. ~~The K$_{soil\_plant}$ and K$_{soil\_root}$ depend strongly on the soil~~

415 ~~water content and the soil hydraulic properties. Therefore, K_{soil_plant} and K_{soil_root} were not only a plant~~

416 ~~property but also a soil property.~~

417 [Insert Figure ~~11~~9 here]

3.3. Relative importance of root and leaf area growth to transpiration and crop performance at canopy

419   **level**

420 Drought stress was observed in the rainfed plot (F2P2) in the second week of June 2017 with mild leaf

421 rolling. The crop then recovered due to sufficient rainfall and lower evaporative demand. Drought stress

422 occurring again at the stem elongation phase caused reduction of plant size (height and stem diameter)

423 (Supplementary material ~~4~~6) as well as a slight reduction of leaf area and biomass in this plot

424 (Supplementary material 3a & 3c). Transpiration per unit of leaf area did not differ much among water

425 treatments and soil types in 2017 (~~Figure~~ Supplementary material S8~~12~~). The opposite was the case for

426 the transpiration rate per unit of root length. The observed root length at different soil depths (Figure 2)

427 and total root length for two plots in the stony soil was much smaller than in the silty soil (Figure 3).

428 Therefore, transpiration per unit of root length in the stony soils (F1P2 & F1P3) was almost 3 times higher

429 than transpiration in the silty soil. For the same soil, transpiration per unit root length of the irrigated

430 treatment was slightly larger than in the rainfed plot.

431   ~~[Insert Figure 12 here]~~

432 The differences in sap flow per plant between water treatments and soil types were more pronounced in

433 2018 (~~Figure~~ Supplementary material S13~~9~~). The highest transpiration rate was observed in the irrigated

434 plots (F1P3 & F2P3), followed by the rainfed plot of the silty soil (F2P2) and it was lowest in the rainfed

435 plot of the stony soil (F1P2). These observations were in line with the differences in biomass and leaf area

436 index between the treatments (Supplementary material 3b & 3d) and plant size (Supplementary material

437 6~~4~~b-c-d). In 2018, severe leaf rolling was observed in the rainfed plot (F1P2) from the beginning of June

438 until the end of the growing period in 2018 (Supplementary material 3d). Similar to 2017, transpiration

439 per unit of root length was much higher in the stony plots as compared to silty plots. Also, for the silty soil,

440 transpiration per unit of root length of the irrigated plot (F2P3) was higher than in the rainfed plot (F2P2).

441 [Insert Figure 13 here]

442 Higher cumulative transpiration in the irrigated plots did not result in higher transpiration use efficiency

443 (TUE) in both soil types (Figure 1410). For instance, TUE were 16.87 g mm^{-1} and 15.59 g mm^{-1} for F1P2 and

444 F2P2, respectively, while they were 15.47 and 14.79 g mm^{-1} for F1P3 and F2P3, respectively, in 2017 (Figure

445 104aA). For the same soil, the rainfed plot showed slightly higher TUE than the irrigated plot. When

446 comparing the TUE of maize of the two soil types for the same water treatment, TUE at the stony soil was

447 almost the same in silty soil. The TUE was not much different among treatments and soil types in 2018.

448 Overall, TUE in 2017 was higher as compared to 2018 (Fig. 104b).

449 [Insert Figure 14 10 here]

450 **4. Discussions**

451 **4.1. Effects of soil types, water application, and climatic condition on root growth**

452 Our root observations showed that soil type considerably affected root growth more than water treatment

453 (Figure 2). Root growth was strongly inhibited by the stony soil where much lower root length was

454 observed than in the silty soil, especially in the deeper soil layers. This was consistent with the findings

455 reported in (Morandage et al., 2021) where a linear increase of stone content resulted in a linear decrease

456 of rooting depth across all stone contents and developmental stages. Also, both simulations and

457 observations indicated that rooting depth was sensitive increased due to the presence of cracks in the

458 lower minirhizontron facility (Morandage et al., 2021) which could explain the high root length between

459 40 and 120 cm soil depths which was observed in the silty soil in both years. In the silty soil, root growth

460 was favored towards deeper soil layers as also reported for the same field in 2016 for winter wheat

461 (Nguyen et al., 2020). Observation in field grown maize, the higher root length density and root diameter
462 were found in the sand than in the loam. This was attributed to the higher investment in nutrient
463 exploration because the lower concentration of plant available nutrients was in sand than in loam
464 (Vetterlein et al., 2022). Also, the larger root diameters in sand than in loam are more likely explained by
465 the need for soil contact of the roots (Jorda et al., 2022; Vetterlein et al., 2022).

466 Our total root length was in the reported range of Cai et al., (2018) who studied winter wheat roots on the
467 same soil types in 2016. The total root length in our work was higher than the reported results from Cai
468 et al., (2018) especially in the rainfed plot of the silty soil (F2P2) in 2018 (Fig. 3). In terms of the root: shoot
469 ratio, our observations were in line with those reported in the same soil types for wheat in Cai et al., (2018).
470 Ordóñez et al., (2020) has reported much larger figures of for instance 880 cm g^{-1} in different locations and
471 under different N application rates in maize growing in the Midwest of US. Jorda et al., (2022) reported a
472 wide range of ratios of root length to shoot biomass root: shoot ratio from 200 to 1000 cm g^{-1} around
473 flowering time of maize depending on the wild type and root hair mutant genotypes growing on either
474 loamy or sandy soils. More roots and higher ratios of root length to shoot biomass root: shoot ratios were
475 found in the sand than in the loam in both wild type and root hair mutant genotypes (Jorda et al., 2022;
476 Vetterlein et al., 2022). Cai et al., (2018) observed much larger ratios of root length to shoot biomass root:
477 shoot ratio in drought stressed plots than in irrigated plot in both soil types in winter wheat which
478 indicated the alternation of sink: source relationships to cope with water stress. This study emphasized
479 that more assimilates are used to promote root growth and extract more water under drought stress.
480 However, this was not the case for the stony soil in our work where the drought stress was more
481 pronounced, especially in 2018. A slightly higher root: shoot ratio in the F1P2 treatment compared to F1P3
482 (DOY 194 & 255) was observed in 2017 while the root: shoot ratio in the two treatments was almost the
483 same on DOY 199 and 228 in 2018 (Fig. 3). We only observed much higher root: shoot ratio in the rainfed
484 plot (F2P2) as compared to the irrigated plot on the silty soil (F2P3). Comas et al., (2013) has reported that

485 ~~maize increases the ratio of root to leaf surface area and relative distribution to deeper depths in~~
486 ~~responses to water deficit. Under drought stress, root growth of maize continues longer into the season~~
487 ~~than shoot and vegetative growth and even beyond the onset of reproduction.~~ A drop of soil water
488 potential (Supplementary material 2b), thus effective soil water potential (Figure ~~8a~~6a) was substantial
489 from 10th July 2018 toward the harvest in the rainfed plot in the silty soil (F2P2) which was consistent with
490 the reduction of leaf water potential (Fig. ~~8b~~6b), leaf area (Supplementary material 3c), total dry matter
491 (Supplementary material 3d), and crop height (Supplementary material ~~4b~~6b) as compared the irrigated
492 plot (F2P3). This indicates a mild water stress in 2018 in the rainfed plots on the silty soil. The larger ratios
493 of root length to shoot biomass ~~root: shoot ratio~~ in this F2P2 plot in 2018 as compared to F2P3 could be
494 explained by the change of source: sink relations where more assimilates were devoted to root growth,
495 even at a later growth stage. Moreover, the low stone content and soil cracks (Morandage et al., 2021)
496 might favor root growth in the deeper soil layers which are close to the ~~lower~~ shallow soil water table in
497 the rhizotrone facility ~~site~~ with silty soil (Vanderborght et al., 2010). In conclusion, both soil texture and
498 water conditions influenced the root growth, however, the effects of the former on root length was more
499 pronounced than the later."

500 **4.2. Effects of soil types, water application, and climatic condition on stomatal conductance,**
501 **photosynthesis, transpiration, leaf water potential, and plant hydraulic conductance**

502 **4.2.1. Leaf water potential and stomatal conductance as affected by soil water conditions**

503 ~~In our study, stomata closed earlier and at more negative soil and leaf water potentials in stony soil than~~
504 ~~in silty soil (see Fig. 4, 5, 6 and 7).~~ In ~~other~~ the previous work, Koehler et al., (2022) reported that maize
505 stomata closed at lower negative leaf water potentials in sand than in loam growing under controlled
506 environment. Cai et al., (2022b) investigated transpiration response of pot-grown maize in two contrasting
507 soil textures (sand and loam) and exposed to two consecutive VPD levels (1.8 and 2.8 kPa). Transpiration
508 rate decreased at less negative soil matric potential in sand than in loam at both VPD levels. In sand, high

509 VPD generated a steeper drop in stomatal conductance with decreasing leaf water potential which

510 indicated that the transpiration and stomatal responses depend on soil hydraulics. In our study, stomata

511 closed earlier and at more negative soil and leaf water potentials in the stony soil than in the silty soil (see

512 Fig. 4, 45, & 6 and 7 and Supplementary material 4 & 5). The lower soil water holding capacity of the stony

513 soil compared to the silty soil resulted in lower soil water potential and smaller total plant hydraulic

514 conductance which in turn led to earlier stomatal closure and to more negative soil water potential in the

515 stony soil.

516 Stomatal control is an early and effective response to water stress to prevent the plant from water loss

517 and dehydration. Maize is considered as an isohydric plant which closes its stomata to maintain leaf water

518 potential above critical levels (Tardieu and Simonneau, 1998). Our results showed that minimum leaf

519 water potential varied among treatments (-1.5 MPa for F1P3, F2P2, and F2P3 and up to -2 MPa for F1P2

520 in 2017, while in 2018 minimum values were -2 MPa for F2P3, F2P2, and F2P3 and -2.7 MPa for F1P2) (Fig.

521 7 5, and Fig. 86, and Fig. 97). Large variability of minimum LWP has been reported for maize genotypes.

522 Leaf water potential can be limited at quite high values, for instance -0.8 MPa in some lines of maize, while

523 values as low as -1.5 MPa have also been recorded (Welcker et al., 2011). Some drought-tolerant maize

524 genotypes close stomata at less negative leaf water potential under soil water depletion than more

525 sensitive ones, which is associated with their ability to avoid xylem embolism and hydraulic failure

526 (Cochard, 2002; Tyree et al., 1986; Li et al., 2009). However, our results show that the leaf water potential

527 threshold can vary within the same genotype depending on soil types, climatic conditions and water

528 management. It should be noted the constant ψ_{leaf} level (around -1.8 MPa) under different soil water

529 regimes reported in Tardieu and Simonneau (1998) that was associated with high VPD values, was based

530 on observations from a single day. Measurements on ψ_{leaf} and Gs for different days during several growing

531 seasons have been rarely reported for maize. The results of our study confirmed that maize appears to

532 maintain its ψ_{leaf} at around -1.5 to -2 MPa which depended on evaporative demand and levels of soil

533 ~~moisture (Fig. 1, Fig. 7, Fig. 8, and Fig. 9). This has been reported recently in Nguyen et al. (2022a). Our~~

534 ~~current study, which investigates the drivers of the modifications of ψ_{leaf} during the growing season, also~~

535 ~~confirmed that such stomatal regulation and the ψ_{leaf} were mediated by soil hydraulics. Cochard, (2002)~~

536 ~~reported that stomatal closure is complete between -1.6 and -2 MPa. In our study, the observed ψ_{leaf} was~~

537 ~~below -2 MPa for several days. Similar values were also reported by Li et al. (2002) for field-grown maize~~

538 ~~in semiarid conditions. In our study, leaf water potential dropped below -2 MPa in the rainfed plots to~~

539 ~~levels much lower than those observed in the irrigated plots in 2018. This could imply different degrees of~~

540 ~~isohydry in maize. A continuum exists in the degree to which stomata regulate the ψ_{leaf} for trees (Domec~~

541 ~~and Johnson, 2012; Klein, 2014) or in grape-vine (Schultz, 2003). Also, cultivars of grape vine show large~~

542 ~~differences in minimum ψ_{leaf} indicating differing degrees of isohydric behavior (Coupel-Ledru et al., 2014).~~

543 ~~When comparing different herbaceous species, Turner et al., (1984) showed that there was a range of~~

544 ~~isohydric behavior among the species in terms of the response to increasing vapor pressure deficit (VPD)~~

545 ~~under sufficient soil moisture. However, conclusions concerning contrasting minimum ψ_{leaf} between 2017~~

546 ~~and 2018 should not be overemphasized. Observed extremely low ψ_{leaf} correspond with the extremely low~~

547 ~~Gs and were further accompanied by complete leaf curling in rainfed treatment under stony soil in 2018~~

548 ~~(Fig. 4, 5, and Fig. 9) due to the extremely dry and hot summer and severe soil dryness~~. In conclusion, our

549 results confirmed that the minimum ψ_{leaf} was influenced by soil types, soil hydraulic conductance, and

550 atmospheric demand.

551 **4.2.2. Hydraulic conductance components as affected by soil water conditions**

552 Estimates of hydraulic components in soil-plant-atmosphere continuum are important not only to

553 understand its underlying relationship to other crop characteristics (stomatal conduct~~ion~~ance,

554 transpiration, and photosynthesis) but also to provide modeling parameters in process-based soil-root-

555 shoot models (Nguyen et al., 2020; Sulis et al., 2019; Nguyen et al., 2022b). Measurement of the

556 components of hydraulic conductance are challenging under field conditions because it requires the

557 estimatione of transpiration and root to leaf water potential gradients. To our knowledge, our results were

558 unique with regard to the dynamics of K_{soil_plant} for field-grown maize on two soil types and under

559 contrasting water, and climate conditions. Our seasonal K_{soil_plant} ranged from 0.12 mm h^{-1} MPa^{-1} to 0.9 mm

560 h^{-1} MPa^{-1} (Fig. 6~~8~~ & Fig. 9~~7~~; Fig. 10~~8~~, and Supplementary material 5~~7~~). Root system hydraulic conductance

561 ranged from 0.26 to 1.47 mm h^{-1} MPa^{-1} (Figure 11~~9~~). Note that the unit of K_{soil_plant} as mm h^{-1} MPa^{-1} could

562 be equivalent to the unit of 10^{-5} h^{-1} if one assumes 1MPa is approximately 10^5 mm in terms of pressure

563 head. Cai et al., (2018) reported root hydraulic conductance in winter wheat from 0.05 ~~x 10^{-5} h^{-1}~~ to 0.5 mm

564 h^{-1} MPa^{-1} ~~x 10^{-5} h^{-1}~~ in two similar soil types. Nguyen et al., (2020) also reported K_{soil_plant} in winter wheat

565 from 0.0625 ~~x 10^{-5} h^{-1}~~ to 0.461 mm h^{-1} MPa^{-1} ~~x 10^{-5} h^{-1}~~. Meunier et al., (2018) focused on estimating the

566 root system hydraulic conductance of maize in a container experiment where the range of K_{soil_plant} was

567 much larger from 0.37 ~~x 10^{-5} h^{-1}~~ to 36 mm h^{-1} MPa^{-1} ~~x 10^{-5} h^{-1}~~ for the plant density of 10 plant m^{-2}. Jorda et

568 al., (2022) estimated root system hydraulic conductance of 0.5 to 1.5 10^{-3} d^{-1} which would be roughly

569 between 2 to 6 mm h^{-1} MPa^{-1} ~~10^{-5} h^{-1}~~. ~~To simulate leaf water potential in the modeling work for field maize,~~

570 ~~Nguyen et al., (2022b) based on assumption that K_{soil_plant} was 0.53 x K_{soil_root}. Such fraction (0.53) was~~

571 ~~consistent with the reported range in our work (0.3-0.8) with average K_{soil_plant} was at half of root system~~

572 ~~hydraulic conductance across treatments.~~ In our work, except the F2P2 in 2018, the stem hydraulic

573 conductance was 10% to 60% higher than root system hydraulic conductance. This is in line with the report

574 from Gallardo et al., (1996) reported that ~~stem hydraulic conductance of wheat was lower than root~~

575 ~~system conductance at around 71 to 91 days after sowing (DAS), but they were similar at 102 DAS. In~~

576 ~~lupine,~~ stem hydraulic conductance of lupin was two times higher than root system conductance

577 regardless of measured days. ~~The larger root length in wheat than lupine did not necessarily result in~~

578 ~~higher root conductance in wheat. Together with this study, our study~~This emphasizes the values of stem

579 hydraulic conductance compared to the root hydraulic conductance in maintaining water potential

580 gradient from shaded leaf or plant color to the sunlit leaf.

581 Our results showed clear differences in K_{soil_plant} among treatments where much lower K_{soil_plant} was

582 observed in the F1P2 as compared to F2P2 (see Figure ~~10~~8 for 2018; Figure ~~6~~8 and ~~9~~7 and Supplementary

583 material ~~5~~7 for both years). This indicated the soil texture dependence for whole plant hydraulic

584 conductance. Maize plants with the shorter root system (i.e. rainfed plot in the stony soil in 2018) (Fig. 3)

585 had lower plant hydraulic conductance. Our results indicated that there was an impact of soil hydraulic

586 conditions on K_{soil_plant} via the reduction of root system hydraulic conductance. Our analysis for three

587 consecutive measurement days in 2018 (Fig ~~10~~8) showed that in the silty soil, K_{soil_plant} decreased when soil

588 water potentials are becoming more negative. For instance, in the silty soil in 2018 when the soil water

589 potentials were considerably lower in the rainfed than in the irrigated plot (e.g. after 10th July), K_{soil_plant}

590 was lower in the rainfed than in the irrigated plot. In the stony soil, the K_{soil_plant} and leaf water potentials

591 seems to decrease more considerably (compared to the silty soil) when the soil water potentials become

592 more negative. In other words, K_{soil_plant} increased considerably when the soil water potentials in the stony

593 soil increased. ~~Koehler et al., (2022) analyzed the maize plant responses to soil drying under controlled~~

594 ~~climate conditions with three soil types (sand, sandy loam, and loam). This study confirmed the impact of~~

595 ~~soil texture on plant response to soil drying in various relationships. In their work, the soil-plant~~

596 ~~conductance decreased in both sand and loam but at less negative water potentials in the sand than in the~~

597 ~~loam. Root system hydraulic conductance decreased at less negative bulk soil water potential in the coarse~~

598 ~~soil than in the fine soil (Vanderborght et al., 2023).~~In our work, K_{soil_plant} increased slowly after irrigation

599 mainly for the severe water stress plot (see F1P2 on 19 July in Fig ~~9d~~7d and ~~10~~8c). This implied that added

600 soil water by irrigation took some time for recovery the soil-root contact within the rhizosphere.

601 **4.2.3. Relationships of stomatal conductance, transpiration, photosynthesis with plant hydraulic**

602 **variables**

603 ~~In 2017, our estimated midday effective soil water potential ($\psi_{soil\_effec\ MD}$) did not vary much (between soil~~

604 ~~types and treatments) which was consistent with the low variability in midday sunlit leaf water potential~~

605 ~~($\psi_{sunlitleaf\ MD}$) and K_{soil_plant} among water treatments (Fig. 8). The $\psi_{soil\_effecMD}$ was high (around -0.35 MPa)~~

606 ~~while $\psi_{sunlitleaf\ MD}$ was around -1.5 MPa (Fig. 8c). In contrast, the difference of $\psi_{soil\_effec\ MD}$, $\psi_{sunlitleaf\ MD}$, and~~

607 ~~K_{soil_plant} was higher among water treatments and soil types in 2018 as compared to 2017. Moreover, the~~

608 ~~high VPD and air temperature in combination with the small precipitation in the main growing season in~~

609 ~~2018 led to a stronger reduction of $\psi_{soil\_effec\ MD}$ up to -0.75 MPa (i.e. in F1P2 in the stony soil on 17 and 18~~

610 ~~July in 2018, Figure 9) and $\psi_{sunlitleaf\ MD}$ to -2.5 MPa. This low $\psi_{soil\_effec\ MD}$ in F1P2 was associated with low~~

611 ~~stomatal conductance (Fig. 9c), low K_{soil_plant} (Fig. 9d), and strong transpiration reduction (Fig. 10a-b, Fig.~~

612 ~~12, and Supplementary material 5). Our results were in line with the analysis from Cai et al., (2022a) which~~

613 ~~revealed that water uptake depended on effective soil water potential which in turn depended on soil~~

614 ~~water potential which differed between plots with different textures.~~

615 The transpiration rate and K_{soil_plant} (slope of linear regression lines in Fig. ~~18~~0a and b) were very low in the

616 rainfed plot under the stony soil (F1P2) which was associated with the large $\psi_{difference}$ (Fig. ~~10a~~8a & b) and

617 the lower stomatal conductance as compared to other plots (Fig. ~~9~~7c). The K_{soil_plant} slightly increased after

618 irrigation (18 July - DOY 199 in Fig. 8~~10~~b) corresponding with the smaller $\psi_{difference}$ (Fig. ~~18~~0b) and an

619 increase in stomatal conductance (Fig. 7~~9~~c). Seasonal K_{soil_plant} was low in the rainfed plot under stony soil

620 (F1P2) with the larger $\psi_{difference}$ (Supplementary material 5~~7~~). In addition, our study showed that the midday

621 stomatal conductance, photosynthesis, and transpiration were significantly correlated only with midday

622 K_{soil_plant} in the rainfed plot on the stony soil (F1P2) in 2018 where high VPD and temperature occurred

623 (Supplementary material 6~~10~~, 11~~7~~, and ~~Supplementary material 8~~12). Maize plants had lower plant

624 hydraulic conductance and more negative soil water potential in the rainfed plot in stony soil ~~required the~~

625 ~~larger gradients in soil water pressure to sustain the same transpiration rate (that~~thus and they exhibited

626 earlier stomatal closure~~)~~ as compared to the same plot in the silty soil. This was in line with a study from

627 Abdalla et al., (2022) which suggested that during soil drying, stomatal regulation of tomato is controlled

628 by root and soil hydraulic conductance. Recent work from Müllers et al., (2022) on faba bean and maize

629 suggested that differences in the stomatal sensitivity among plant species can be partly explained by the

630 sensitivity of soil-plant hydraulic conductance to soil drying. The loss of conductance has immediate

631 consequences for leaf water potential and the associated stomatal regulation. Cai et al., (2022b) also

632 showed that the decrease in sunlit leaf stomatal conductance was well correlated with the drop in soil-

633 plant hydraulic conductance, which was significantly affected by soil texture. This was confirmed in our

634 work where the stony soil strongly impacted on root growth, modulated $K_{soil\_plant,}$ and consequently

635 influenced the leaf stomatal conductance, photosynthesis, and transpiration.

636 **4.3. Relative contribution of water control by leaves and roots on transpiration and transpiration use**

637 **efficiency**

638 Responses of crops via stomatal control to reduce water loss at leaf scale while maintaining leaf

639 photosynthesis and water use efficiency were reported earlier (Nguyen et al., 2022a; Vitale et al., 2007).

640 In addition to that, in the maize experiments in 2017 and 2018In our study, leaf rolling was observed in

641 both rainfed plots on the stony and the silty soil in the second week of June 2017 and from the beginning

642 of June until the end of the growing period in 2018. This indicates another dehydration avoidance

643 mechanism resulting from morphological adjustments which is an effective mechanism for delaying

644 senescence (Aparicio-Tejo and Boyer, 1983; Richards et al., 2002). Stomatal closure resulted in more

645 reduction of transpiration and assimilation in the rainfed plots than irrigated plots with the same soil type

646 (Fig. 54, Supplementary material Fig. 64 & 5, Fig. 75, and Fig. 13Supplementary material 9Aa). There was

647 reduction of shoot biomass (also stem size and leaf size adjustments) in F1P2 as compared to other plots.

648 However, the TUE was not smaller in this plot than the remaining plots. These observations confirm that

649 plant size adjustments through reduction of height, leaf width and length are efficient responses to reduce

650 water loss at canopy scale in addition to stomatal control at the leaf level.

651 Relative contribution of leaf area to transpiration has been highlighted in wheat where reduction of tiller

652 number resulted in significantly (lower LAI, thus lower canopy transpiration (Cai et al., 2018; Trillo and

653 Fernández, 2005; Nguyen et al., 2022a). However, root system conductance per unit of leaf area and per

654 unit root mass were strongly reduced and eventually more than reduction of leaf area under water stress

655 (Trillo and Fernández, 2005). In our work, expressing the transpiration per unit of root length on the one

656 hand allowed to analyze the role of total root length to water uptake. However, on the other hand, the

657 lower total root length did not necessarily result in a lower root water uptake and vice versa. For instance,

658 the rainfed plot of the treatment F2P2 had the larger total root length which could postpone the effect of

659 soil water limitations in drying soils due to greater ability to extract water from subsoils. Therefore,

660 transpiration was very similar between F2P2 and F2P3. Despite of the much lower total root length in the

661 stony soil, K_{soil_plant} in the irrigated plot (F1P3) was not much lower than in the same water treatment in

662 the silty soil (F2P3, Fig. 6~~8c~~d, 9~~7c~~d, Fig. ~~10~~8, and Supplementary material ~~5~~7). This could be explained by

663 the fact that the K_{soil_plant} variability was not only depended on root architecture (here the root length and

664 distribution) but also depended on the variability of root segment hydraulic properties which has also been

665 illustrated and discussed in Zwieniecki et al. (2002), Frensch and Steudle (1989), Meunier et al. (2018),

666 Couvreur et al. (2014), and Ahmed et al. (2018). ~~Meunier et al. (2020) showed that more than 65% of the~~

667 ~~variability of root system conductance of maize plants could be attributed to variability in root~~

668 ~~architecture, which includes root length, whereas only 25% of the variability was attributed to root~~

669 ~~segment hydraulic properties. However, the analysis of Meunier et al., (2020) neither included the impact~~

670 ~~of root hairs nor the impact of rhizosphere conductivity but only focused on the root system hydraulic~~

671 ~~conductance.~~ Moreover, the contribution of shoot hydraulic conductance could be large in plants (Gallardo

672 et al., 1996; Trillo and Fernández, 2005; Sunita et al., 2014) which also confirmed in our work. In our work,

673 K_{soil_plant} comprised root and shoot conductance which are directly influenced by soil hydraulics. Our

674 estimates of K_{soil_plant} varied with transpiration and gradients of $\psi_{sunlitleaf}$ and ψ_{soil_effec}. Thus, any change of

675 soil hydraulic conductance will change the root to shoot water potential. Consequently, it will affect the

676 gradients between shoot and root rhizosphere (Carminati and Javaux, 2020). Thus, our study illustrate~~s is~~

677 ~~revealing~~ the importance of both soil texture characteristics and root phenotypic traits (here root length)

678   in regulating plant transpiration (Cai et al., 2022a). Other traits like root hair density (Cai et al., 2022a) or

679   higher root length density (Vadez, 2014) could contribute to the soil to root water potential and root-zone

680   hydraulic conductance where dense root hairs ~~are delaying~~delayed soil water deficit in drying soils.

681   However, contrasting results have shown that root hairs did not have an effect~~s~~ on root water uptake (see

682   Jorda et al. 2022). The role of root hairs could not be analyzed in our work which was based on the root

683   data from minirhizotron images.

5. Conclusion

685   We presented plant hydraulic characteristics and crop growth from root to shoot of maize under field-

686   grown conditions with two soil types (silty and stony), each soil with two water regimes (irrigated and

687   rainfed) for two growing seasons (2017, 2018). Our results confirmed that root length and ratios of root

688   length to shoot biomass~~root: shoot ratio~~ ~~was~~ were modulated by soil types and water treatment but less

689   by seasonal evaporative demand. Increase ratio of root length to shoot biomass~~root: shoot ratio~~ has been

690   an important response of maize that allows plants to extract more water under drought stress that

691   occurred rather in the silty soil but less in the stony soil due to the higher content of stony material. Despite

692   of lower root length in the stony irrigated plot, transpiration rate was not much lower than in the silty

693   irrigated plot. This could be related to another property of the root such as root segment conductance or

694   other root traits (e.g. root hair). Further investigation with extensive measurements of roots including axial

695   and radial root conductance at field scale will be required to better explain the observed results.

696   Another conclusion is that stomatal regulation maintains leaf water potential at certain thresholds which

697   depends on soil types, soil water availability, and seasonal atmospheric demand. The stomata conductance

698   was smaller and decreased at more negative leaf water potentials in stony soil than in silty soil. The leaf

699   water potentials are affected by the soil-plant ~~plant~~ hydraulic conductance. In addition to stomatal

700   regulation, leaf growth and plant size adjustments are important to regulate the transpiration ~~that~~ and

701   water use efficiency ~~was not different among treatments and soil types~~ in the same year.

702 The lowest soil-plant hydraulic conductance was observed in the stony soil with severe drought stress as

703 compared to silty soil while its variation depends also on the soil water variation (before and after

704 irrigation). Root system and soil-plant hydraulic conductance depended strongly on soil hydraulic

705 properties. In the stony soil, which has a considerably smaller water holding capacity than the silty soil,

706 root length was considerably smaller than in the silty soil. Nevertheless water uptake per unit root length

707 was much larger than in the fine soil. This also means that the hydraulic conductance per unit root length

708 must have been much larger in the stony soil than in the fine soil. Cai et al., (2018) observed a similar effect

709 for winter wheat but they found much smaller differences in the root length normalized root conductance.

710 The higher root length normalized root conductance means that the anatomy of the root tissues must

711 have been influenced by the soil texture and compensated the considerably smaller root length in the

712 stony soil. Looking at the effect of water treatments in the silt soil, the non-irrigated plot had more roots

713 than the irrigated one and both had more roots in the year with high VPD. But the soil-root conductance

714 was higher in the irrigated plot than in the rainfed plot. This means that in the irrigated plot, the soil-root

715 conductance per unit root length was higher than in the rainfed plot. This could either be due to wetter

716 soil conditions and higher soil conductance or it could be due to a larger conductance of the root tissues.

717 Especially in 2017 when the silty soil was wetter, the slightly larger soil-root conductance in the irrigated

718 plot is most likely the result of larger root tissue conductance in the irrigated plot. Thus, how root

719 architecture (here represented simply by the total root length) and root tissue conductivities 'respond' to

720 drought stress might be opposite depending on the comparisons that are made. When the stony soil and

721 silt soil are compared, the higher 'stress' due to lower water availability in the stony soil resulted in less

722 roots with a higher root tissue conductance in the soil with more stress. When comparing the rainfed with

723 the irrigated plot in the silty soil, the higher stress in the rainfed soil resulted in more roots with a lower

724 root tissue conductance in the treatment with more stress. This illustrates that the 'response' to stress can

725 be completely opposite depending on conditions or treatments that lead to the differences in stress that

726 are compared. Therefore, it cannot be the 'stress' alone that defines how a plant will react and adapt its

727 root system. Modelling the impact of stress and the feedback between drought stress and plant

728 development is likely controlled by other properties or parameters that change with changing soil water

729 availability and atmospheric water demand then the plant stress level. Results from this study show that

730 soil-crop models should focus not only on simulating stomatal regulations to capture the response to

731 drought stress, but also require adequate representations of leaf growth and adjustments.

732

733

734

735

736

737 **Acknowledgements**

738 This work has partially been funded by Federal Ministry of Education and Research (BMBF) through

739 European SUSCAP project – 031B0170B and COINS project) and the Deutsche Forschungsgemeinschaft

740 (DFG, German Research Foundation) under Germany's Excellence Strategy – EXC 2070 – 390732324". We

741 acknowledge the support by the SFB/TR32 "Pattern in Soil–Vegetation–Atmosphere Systems: Monitoring,

742 Modelling, and Data Assimilation" funded by the Deutsche Forschungsgemeinschaft (DFG). Thuy Nguyen

743 and Thomas Gaiser also thank the DETECT – CRC 1502 research program which is funded by DFG. We thank

744 Dr. Matthias Langensiepen for his supports and technical help in the TR32 project. We would like to thank

745 all the student assistants and technicians for their considerable efforts to collect the data in the field and

746 the laboratories.

747

748

749

750

751

752

753

754

755

756

757

List of Tables

Table 1. Crop phenology and management information for different treatments in 2017 and 2018.

	2017				2018			
Soil types	Stony (F1)	Stony (F1)	Silty (F2)	Silty (F2)	Stony (F1)	Stony (F1)	Silty (F2)	Silty (F2)
Water treatments	Rainfed (P2)	Irrigated (P3)	Rainfed (P2)	Irrigated (P3)	Rainfed (P2)	Irrigated (P3)	Rainfed (P2)	Irrigated (P3)
Plot names	F1P2	F1P3	F2P2	F2P3	F1P2	F1P3	F2P2	F2P3
Growing season (days)$^{¥}$	136	136	136	136	107	107	107	107
Cumulative rainfall (mm)*	248.7	248.7	248.7	248.7	91.3	91.3	91.3	91.3
Irrigation (mm)	0	130	0	130	66	257.6	0	257.6
Fertilizer application (mm/dd) (per hectare)	05/09:100 kg N + 40kg P_2O_5 07/06: 80 kg N + 40 kg K_2O				05/22: 100 kg N 05/30: 40 kg P_2O_5 + 40 kg K_2O 06/27: 80 kg N			
Sowing date (mm/dd)	05/04				05/08			
Emergence date	05/09				05/13			
Tasseling date	07/09				07/09			
Silking date	07/14				07/11			
Harvest date	09/12				08/22			

760   Notes: ¥ from sowing to harvest; * for rainfall for whole growing season;

761

762

763

764

765

766

767

768

769

770   **Reference**

771   Abdalla, M., M.A. Ahmed, G. Cai, F. Wankmüller, N. Schwartz, et al. 2022. Stomatal closure during water
772   deficit is controlled by below-ground hydraulics. Ann. Bot. 129(2): 161–170. doi:
773   10.1093/aob/mcab141.

774   Abdalla, M., A. Carminati, G. Cai, M. Javaux, and M.A. Ahmed. 2021. Stomatal closure of tomato under
775   drought is driven by an increase in soil-root hydraulic resistance. Plant. Cell Environ. 44(2): 425–
776   431. doi: 10.1111/pce.13939.

777   Ahmed, M.A., M. Zarebanadkouki, F. Meunier, M. Javaux, A. Kaestner, et al. 2018. Root type matters:
778   Measurement of water uptake by seminal, crown, and lateral roots in maize. J. Exp. Bot. 69(5): 1199–
779   1206. doi: 10.1093/jxb/erx439.

780   Aparicio-Tejo, P., and J.S. Boyer. 1983. Significance of Accelerated Leaf Senescence at Low Water Potentials
781   for Water Loss and Grain Yield in Maize1. Crop Sci. 23(6): cropsci1983.0011183X002300060040x. doi:
782   https://doi.org/10.2135/cropsci1983.0011183X002300060040x.

783   Bauer, F.M., L. Lärm, S. Morandage, G. Lobet, J. Vanderborght, et al. 2021. Combining deep learning and
784   automated feature extraction to analyze minirhizotron images: development and validation of a new
785   pipeline.   bioRxiv   (1):   2021.12.01.470811.
786   https://www.biorxiv.org/content/10.1101/2021.12.01.470811v1%0Ahttps://www.biorxiv.org/cont
787   ent/10.1101/2021.12.01.470811v1.abstract.

788   Bornemann*, L., M. Herbst, G. Welp, H. Vereecken, and W. Amelung. 2011. Rock Fragments Control Size
789   and Saturation of Organic Carbon Pools in Agricultural Topsoil. Soil Sci. Soc. Am. J. 75(5): 1898. doi:

790   10.2136/sssaj2010.0454.

791   Bourbia, I., C. Pritzkow, and T.J. Brodribb. 2021. Herb and conifer roots show similar high sensitivity to
792   water deficit. Plant Physiol. 186(4): 1908–1918. doi: 10.1093/plphys/kiab207.

793   Cai, G., M.A. Ahmed, M. Abdalla, and A. Carminati. 2022a. Root hydraulic phenotypes impacting water
794   uptake in drying soils. Plant Cell Environ. 45(3): 650–663. doi: 10.1111/pce.14259.

795   Cai, G., M. König, A. Carminati, M. Abdalla, M. Javaux, et al. 2022b. Transpiration response to soil drying
796   and vapor pressure deficit is soil texture specific. Plant Soil (0123456789). doi: 10.1007/s11104-022-
797   05818-2.

798   Cai, G., J. Vanderborght, V. Couvreur, C.M. Mboh, and H. Vereecken. 2017a. Parameterization of Root
799   Water Uptake Models Considering Dynamic Root Distributions and Water Uptake Compensation.
800   Vadose Zo. J. 0(0): 0. doi: 10.2136/vzj2016.12.0125.

801   Cai, G., J. Vanderborght, A. Klotzsche, J. van der Kruk, J. Neumann, et al. 2016. Construction of
802   Minirhizotron Facilities for Investigating Root ZoneProcesses. Vadose Zo. J. 15(9): 0. doi:
803   10.2136/vzj2016.05.0043.

804   Cai, G., J. Vanderborght, M. Langensiepen, A. Schnepf, H. Hüging, et al. 2018. Root growth, water uptake,
805   and sap flow of winter wheat in response to different soil water conditions. Hydrol. Earth Syst. Sci.
806   22(4): 2449–2470. doi: 10.5194/hess-22-2449-2018.

807   Cai, Q., Y. Zhang, Z. Sun, J. Zheng, W. Bai, et al. 2017b. Morphological plasticity of root growth under mild
808   water stress increases water use efficiency without reducing yield in maize. Biogeosciences 14(16):
809   3851–3858. doi: 10.5194/bg-14-3851-2017.

810   Carminati, A., and M. Javaux. 2020. Soil Rather Than Xylem Vulnerability Controls Stomatal Response to
811   Drought. Trends Plant Sci. 25(9): 868–880. doi: 10.1016/j.tplants.2020.04.003.

812   Carminati, A., M. Zarebanadkouki, E. Kroener, M.A. Ahmed, and M. Holz. 2016. Biophysical rhizosphere
813   processes affecting root water uptake. Ann. Bot. 118(4): 561–571. doi: 10.1093/aob/mcw113.

814   Choudhary, S., and T.R. Sinclair. 2014. Hydraulic conductance differences among sorghum genotypes to
815   explain variation in restricted transpiration rates. Funct. Plant Biol. 41(3): 270–275. doi:
816   10.1071/FP13246.

817   Cochard, H. 2002. Xylem embolism and drought-induced stomatal closure in maize. Planta 215(3): 466–
818   471. doi: 10.1007/s00425-002-0766-9.

819   Comas, L.H., S.R. Becker, V.M. V. Cruz, P.F. Byrne, and D.A. Dierig. 2013. Root traits contributing to plant
820   productivity under drought. Front. Plant Sci. 4(NOV): 1–16. doi: 10.3389/fpls.2013.00442.

821   Coupel-Ledru, A., É. Lebon, A. Christophe, A. Doligez, L. Cabrera-Bosquet, et al. 2014. Genetic variation in
822   a grapevine progeny (Vitis vinifera L. cvs GrenachexSyrah) reveals inconsistencies between
823   maintenance of daytime leaf water potential and response of transpiration rate under drought. J.
824   Exp. Bot. 65(21): 6205–6218. doi: 10.1093/jxb/eru228.

825   Couvreur, V., J. Vanderborght, X. Draye, and M. Javaux. 2014. Dynamic aspects of soil water availability for
826   isohydric plants: Focus on root hydraulic resistances. water Resour. Res. 50: 8891–8906. doi:
827   10.1002/2014WR015608.Received.

828   Couvreur, V., J. Vanderborght, and M. Javaux. 2012. A simple three-dimensional macroscopic root water
829   uptake model based on the hydraulic architecture approach. Hydrol. Earth Syst. Sci. 16: 2957–2971.

830   doi: 10.5194/hess-16-2957-2012.

831 Daryanto, S., L. Wang, and P. Jacinthe. 2016. Global Synthesis of Drought Effects on Maize and Wheat
832   Production. PLoS One 11(5): 1–15. doi: 10.1371/journal.pone.0156362.

833 Draye, X., Y. Kim, G. Lobet, and M. Javaux. 2010. Model-assisted integration of physiological and
834   environmental constraints affecting the dynamic and spatial patterns of root water uptake from
835   soils. J. Exp. Bot. 61(8): 2145–2155. doi: 10.1093/jxb/erq077.

836 Domec, J., and D.M. Johnson. 2012. Does homeostasis or disturbance of homeostasis in minimum leaf
837   water potential explain the isohydric versus anisohydric behavior of Vitis vinifera L . cultivars ? Tree
838   32: 245–248. doi: 10.1093/treephys/tps013.

839 Domec, J., and M.L. Pruyn. 2008. Bole girdling affects metabolic properties and root , trunk and branch
840   hydraulics of young ponderosa pine trees. Tree Physiol. (28): 1493–1504.

841 Dynamax. 2007. Dynagage Sap Flow Sensor User Manual. 1–107. Last access on March 5th 2015.

842 Effendi, R., S.B. Priyanto, M. Aqil, and M. Azrai. 2019. Drought adaptation level of maize genotypes based
843   on leaf rolling, temperature, relative moisture content, and grain yield parameters. IOP Conf. Ser.
844   Earth Environ. Sci. 270(1). doi: 10.1088/1755-1315/270/1/012016.

845 Fang, J., and Y. Su. 2019. Effects of Soils and Irrigation Volume on Maize Yield, Irrigation Water Productivity,
846   and Nitrogen Uptake. Sci. Rep. 9(1): 1–11. doi: 10.1038/s41598-019-41447-z.

847 Frensch, J., and E. Steudle. 1989. Axial and Radial Hydraulic Resistance to Roots of Maize (Zea mays L.).
848   Plant Physiol. 91: 719–726.

849 Gallardo, M., J. Eastham, P.J. Gregory, and N.C. Turner. 1996. A comparison of plant hydraulic
850   conductances in wheat and lupins. J. Exp. Bot. 47(295): 233–239. doi: 10.1093/jxb/47.2.233.

851 Hochberg, U., F.E. Rockwell, N.M. Holbrook, and H. Cochard. 2018. Iso/Anisohydry: A Plant–Environment
852   Interaction Rather Than a Simple Hydraulic Trait. Trends Plant Sci. 23(2): 112–120. doi:
853   10.1016/j.tplants.2017.11.002.

854 Hopmans, J.W., and K.L. Bristow. 2002. Current Capabilities and Future Needs of Root Water and
855   Nutrient Uptake Modeling. In: Sparks, D.L.B.T.-A. in A., editor, Advances in Agronomy. Academic
856   Press. p. 103–183

857 Hubbard, R.M., M.G. Ryan, V. Stiller, and J.S. Sperry. 2001. Stomatal conductance and photosynthesis vary
858   linearly with plant hydraulic conductance in ponderosa pine. Plant, Cell Environ. 24(1): 113–121. doi:
859   10.1046/j.1365-3040.2001.00660.x.

860 IPCC. 2022. Impacts, Adaptation, and Vulnerability. Working Group II Contribution to the IPCC Sixth
861   Assessment Report of the Intergovernmental Panel on Climate Change.

862 Jorda, H., M.A. Ahmed, M. Javaux, A. Carminati, P. Duddek, et al. 2022. Field scale plant water relation of
863   maize (Zea mays) under drought – impact of root hairs and soil texture. Plant Soil 478(1–2): 59–84.
864   doi: 10.1007/s11104-022-05685-x.

865 Klein, T. 2014. The variability of stomatal sensitivity to leaf water potential across tree species indicates a
866   continuum between isohydric and anisohydric behaviours. Funct. Ecol.: 1313–1320. doi:
867   10.1111/1365-2435.12289.

868 Koehler, T., D.S. Moser, Á. Botezatu, T. Murugesan, S. Kaliamoorthy, et al. 2022. Going underground: soil

869 hydraulic properties impacting maize responsiveness to water deficit. Plant Soil 478(1–2): 43–58. doi:
870   10.1007/s11104-022-05656-2.

871 Lärm, L., F.M. Bauer, N. Hermes, J. van der Kruk, H. Vereecken, et al. 2023. Multi-year belowground data
872   of minirhizotron facilities in Selhausen. Sci. Data 10(1): 1–15. doi: 10.1038/s41597-023-02570-9.

873 Li, X., T.R. Sinclair, and L. Bagherzadi. 2016. Hydraulic Conductivity Changes in Soybean Plant-Soil System
874   with Decreasing Soil Volumetric Water Content. J. Crop Improv. 30(6): 713–723. doi:
875   10.1080/15427528.2016.1231729.

876 Li, Y., J.S. Sperry, and M. Shao. 2009. Hydraulic conductance and vulnerability to cavitation in corn (Zea
877   mays L.) hybrids of differing drought resistance. Environ. Exp. Bot. 66(2): 341–346. doi:
878   10.1016/j.envexpbot.2009.02.001.

879 Marin, M., D.S. Feeney, L.K. Brown, M. Naveed, S. Ruiz, et al. 2021. Significance of root hairs for plant
880   performance under contrasting field conditions and water deficit. Ann. Bot. 128(1): 1–16. doi:
881   10.1093/aob/mcaa181.

882 Meunier, F., A. Heymans, X. Draye, V. Couvreur, M. Javaux, et al. 2020. MARSHAL, a novel tool for virtual
883   phenotyping of maize root system hydraulic architectures. In Silico Plants 2(1): 1–15. doi:
884   10.1093/insilicoplants/diz012.

885 Meunier, F., M. Zarebanadkouki, M.A. Ahmed, A. Carminati, V. Couvreur, et al. 2018. Hydraulic
886   conductivity of soil-grown lupine and maize unbranched roots and maize root-shoot junctions. J.
887   Plant Physiol. 227(February): 31–44. doi: 10.1016/j.jplph.2017.12.019.

888 Morandage, S., J. Vanderborght, M. Zörner, G. Cai, D. Leitner, et al. 2021. Root architecture development
889   in stony soils. Vadose Zo. J. (April): 1–17. doi: 10.1002/vzj2.20133.

890 Müllers, Y., J.A. Postma, H. Poorter, and D. van Dusschoten. 2022. Stomatal conductance tracks soil-to-leaf
891   hydraulic conductance in faba bean and maize during soil drying. Plant Physiol. doi:
892   10.1093/plphys/kiac422.

893 Nguyen, T.H., M. Langensiepen, T. Gaiser, H. Webber, H. Ahrends, et al. 2022a. Responses of winter wheat
894   and maize to varying soil moisture: From leaf to canopy. Agric. For. Meteorol. 314(December 2021):
895   108803. doi: 10.1016/j.agrformet.2021.108803.

896 Nguyen, T.H., M. Langensiepen, H. Hueging, T. Gaiser, S.J. Seidel, et al. 2022b. Expansion and evaluation
897   of two coupled root–shoot models in simulating CO2 and H2O fluxes and growth of maize. Vadose
898   Zo. J. 21(3): 1–31. doi: 10.1002/vzj2.20181.

899 Nguyen, T.H., M. Langensiepen, J. Vanderborght, H. Hüging, C.M. Mboh, et al. 2020. Comparison of root
900   water uptake models in simulating CO2 and H2O fluxes and growth of wheat. Hydrol. Earth Syst. Sci.
901   (24): 4943–4969. doi: 10.5194/hess-24-4943-2020.

902 Ordóñez, R.A., S. V. Archontoulis, R. Martinez-Feria, J.L. Hatfield, E.E. Wright, et al. 2020. Root to shoot
903   and carbon to nitrogen ratios of maize and soybean crops in the US Midwest. Eur. J. Agron. 120(June):
904   126130. doi: 10.1016/j.eja.2020.126130.

905 Passioura, J.B., 2006. The perils of pot experiments. Funct. Plant Biol. 33 (12), 1075–1079.
906   https://doi.org/10.1071/FP06223.

907 Ranawana SRWMCJK, Siddique KHM, Palta JA et al (2021) Stomata coordinate with plant hydraulics to
908   regulate transpiration response to vapour pressure defcit in wheat. Functional Plant Biol 48:839–850.

909   https://doi.org/10.1071/FP20392

910   Richards, R.A., G.J. Rebetzke, A.G. Condon, and A.F. van Herwaarden. 2002. Breeding Opportunities for
911   Increasing the Efficiency of Water Use and Crop Yield in Temperate Cereals. Crop Sci. 42(1): 111–
912   121. doi: 10.2135/cropsci2002.1110.

913   Rodriguez-Dominguez, C.M., and T.J. Brodribb. 2019. Declining root water transport drives stomatal
914   closure in olive under. New Phytol. 225: 126–134.

915   Sinclair, T.R., and M.M. Ludlow. 1986. Influence of soil water supply on the plant water balance of four
916   tropical grain legumes. Aust. J. Plant Physiol. 13: 329–341.

917   Scharwies, J.D., and J.R. Dinneny. 2019. Water transport, perception, and response in plants. J. Plant Res.
918   132(3): 311–324. doi: 10.1007/s10265-019-01089-8.

919   Schultz, H.R. 2003. Differences in hydraulic architecture account for near-isohydric and anisohydric
920   behaviour of two field-grown Vitis vinifera L. cultivars during drought. Plant, Cell Environ. 26(8):
921   1393–1405. doi: 10.1046/j.1365-3040.2003.01064.x.

922   Stadler, A., S. Rudolph, M. Kupisch, M. Langensiepen, J. van der Kruk, et al. 2015. Quantifying the effects
923   of soil variability on crop growth using apparent soil electrical conductivity measurements. Eur. J.
924   Agron. 64: 8–20. doi: 10.1016/j.eja.2014.12.004.

925   Sulis, M., V. Couvreur, J. Keune, G. Cai, I. Trebs, et al. 2019. Incorporating a root water uptake model based
926   on the hydraulic architecture approach in terrestrial systems simulations. Agric. For. Meteorol. 269–
927   270: 28–45. doi: https://doi.org/10.1016/j.agrformet.2019.01.034.

928   Sunita, C., T.R. Sinclair, C.D. Messina, and M. Cooper. 2014. Hydraulic conductance of maize hybrids
929   differing in transpiration response to vapor pressure deficit. Crop Sci. 54(3): 1147–1152. doi:
930   10.2135/cropsci2013.05.0303.

931   Tardieu, F., X. Draye, and M. Javaux. 2017. Root Water Uptake and Ideotypes of the Root System: Whole-
932   Plant Controls Matter. Vadose Zo. J. 16(9): 0. doi: 10.2136/vzj2017.05.0107.

933   Tardieu, F., and T. Simonneau. 1998. Variability among species of stomatal control under fluctuating soil
934   water status and evaporative demand: modelling isohydric and anisohydric behaviours. J. Exp. Bot.
935   49(March): 419–432. doi: 10.1093/jxb/49.Special_Issue.419.

936   Tardieu, F. 2016. Too many partners in root – shoot signals . Does hydraulics qualify as the only signal
937   that feeds back over time for reliable stomatal. New Phytol. 212: 802–804.

938   Trillo, N., and R.J. Fernández. 2005. Wheat plant hydraulic properties under prolonged experimental
939   drought: Stronger decline in root-system conductance than in leaf area. Plant Soil 277(1–2): 277–
940   284. doi: 10.1007/s11104-005-7493-5.

941   Tsuda, M., and M.T. Tyree. 1997. Whole-plant hydraulic resistance and vulnerability segmentation in
942   Acer saccharinum. Tree Physiol. (17): 351–357.

943   Turner, N.C., E.D. Schulze, and T. Gollan. 1984. The responses of stomata and leaf gas exchange to vapour
944   pressure deficits and soil water content - I. Species comparisons at high soil water contents.
945   Oecologia 63(3): 338–342. doi: 10.1007/BF00390662.

946   Tyree, M.T., E.L. Fiscus, S.D. Wullschleger, and M.A. Dixon. 1986. Detection of Xylem Cavitation in Corn
947   under Field Conditions. Plant Physiol. 82(2): 597–599. doi: 10.1104/pp.82.2.597.

948 Vadez, V. 2014. Root hydraulics : The forgotten side of roots in drought adaptation. F. Crop. Res. 165: 15–
949   24.

950 Vadez, V., S. Choudhary, J. Kholová, C.T. Hash, R. Srivastava, et al. 2021. Transpiration efficiency: Insights
951   from comparisons of C4cereal species. J. Exp. Bot. 72(14): 5221–5234. doi: 10.1093/jxb/erab251.

952 Vanderborght, J., V. Couvreur, F. Meunier, A. Schnepf, H. Vereecken, et al. 2021. From hydraulic root
953   architecture models to macroscopic representations of root hydraulics in soil water flow and land
954   surface models. Hydrol. Earth Syst. Sci. 25(9): 4835–4860. doi: 10.5194/hess-25-4835-2021.

955 Vanderborght, J., A. Graf, C. Steenpass, B. Scharnagl, N. Prolingheuer, et al. 2010. Within-Field Variability
956   of Bare Soil Evapora Ө on Derived from Eddy Covariance Measurements. Vadose Zo. J. 9: 943–954.
957   doi: 10.2136/vzj2009.0159.

958 Vereecken, H., A. Schnepf, J.W. Hopmans, M. Javaux, D. Or, et al. 2016. Modeling Soil Processes: Review,
959   Key Challenges, and New Perspectives. Vadose Zo. J. 15(5): vzj2015.09.0131. doi:
960   10.2136/vzj2015.09.0131.

961 Vetterlein, D., M. Phalempin, E. Lippold, S. Schlüter, S. Schreiter, et al. 2022. Root hairs matter at field
962   scale for maize shoot growth and nutrient uptake, but root trait plasticity is primarily triggered by
963   texture and drought. Plant Soil 478(1–2): 119–141. doi: 10.1007/s11104-022-05434-0.

964 Vitale, L., P. Di Tommasi, C. Arena, A. Fierro, A. Virzo De Santo, et al. 2007. Effects of water stress on gas
965   exchange of field grown Zea mays L. in Southern Italy: An analysis at canopy and leaf level. Acta
966   Physiol. Plant. 29(4): 317–326. doi: 10.1007/s11738-007-0041-6.

967 Wang, N., J. Gao, and S. Zhang. 2017. Overcompensation or limitation to photosynthesis and root hydraulic
968   conductance altered by rehydration in seedlings of sorghum and maize. Crop J. 5(4): 337–344. doi:
969   10.1016/j.cj.2017.01.005.

970 Weihermüller, L., Huisman, J. A., Lambot, S., Herbst, M., & Vereecken, H. (2007). Mapping the spatial
971   variation of soil water content at the field scale with different ground penetrating radar techniques.
972   Journal of Hydrology, 340, 205–216. https://doi.org/10.1016/j.jhydrol.2007. 04.013

973 Welcker, C., W. Sadok, G. Dignat, M. Renault, S. Salvi, et al. 2011. A common genetic determinism for
974   sensitivities to soil water deficit and evaporative demand: Meta-analysis of quantitative trait loci and
975   introgression lines of maize. Plant Physiol. 157(2): 718–729. doi: 10.1104/pp.111.176479.

976 Zhuang, J., Y. Jin, and T. Miyazaki. 2001. ESTIMATING WATER RETENTION CHARACTERISTIC FROM SOIL
977   PARTICLE-SIZE DISTRIBUTION USING A NON-SIMILAR MEDIA CONCEPT. Soil Sci. 166(5).
978   https://journals.lww.com/soilsci/Fulltext/2001/05000/ESTIMATING_WATER_RETENTION_CHARACT
979   ERISTIC_FROM.2.aspx.

980 Zwieniecki, M.A., P.J. Melcher, C.K. Boyce, L. Sack, and N.M. Holbrook. 2002. Hydraulic architecture of leaf
981   venation in Laurus nobilis L. Plant, Cell Environ. 25(11): 1445–1450. doi: 10.1046/j.1365-
982   3040.2002.00922.x.

983

984

985

Formatted: German (Germany)

986

987

988

989

990

991

992

993

994

995

996

997

Author contribution

Huu Thuy Nguyen, Thomas Gaiser, Jan Vanderborght, and Frank Ewert: Conceptualization; Huu Thuy Nguyen, and Hubert Hüging: Data curation and data quality check (aboveground measurements); Lena Lärm, Felix Bauer, Anja Klotzsche, Jan Vanderborght, and Andrea Schnepf: data curation and data quality check (belowground measurements); Huu Thuy Nguyen: Formal data analysis and visualization; Thomas Gaiser, Jan Vanderborght, Andrea Schnepf, and Frank Ewert: Funding acquisition & Project administration; Huu Thuy Nguyen: writing – original draft; all authors: review, editing, and finalizing the manuscript.

Competing interests

This manuscript has not been published and is not under consideration for publication in any other journal. All authors agreed and approved the manuscript and its submission to this journal. We declare there is no conflict of interest.

Code/Data availability

The meteorological data were collected from a weather station in Selhausen (Germany) which belongs to the TERENO network of terrestrial observatories. Weather data are freely available from the TERENO data portal (https://www.tereno.net/ddp/dispatch?searchparams=freetext-Selhausen, last access: October 2020) (TERENO, 2020). The data which were obtained from the minirhizotron facilities (under- and aboveground) are available from the corresponding author on reasonable requests.
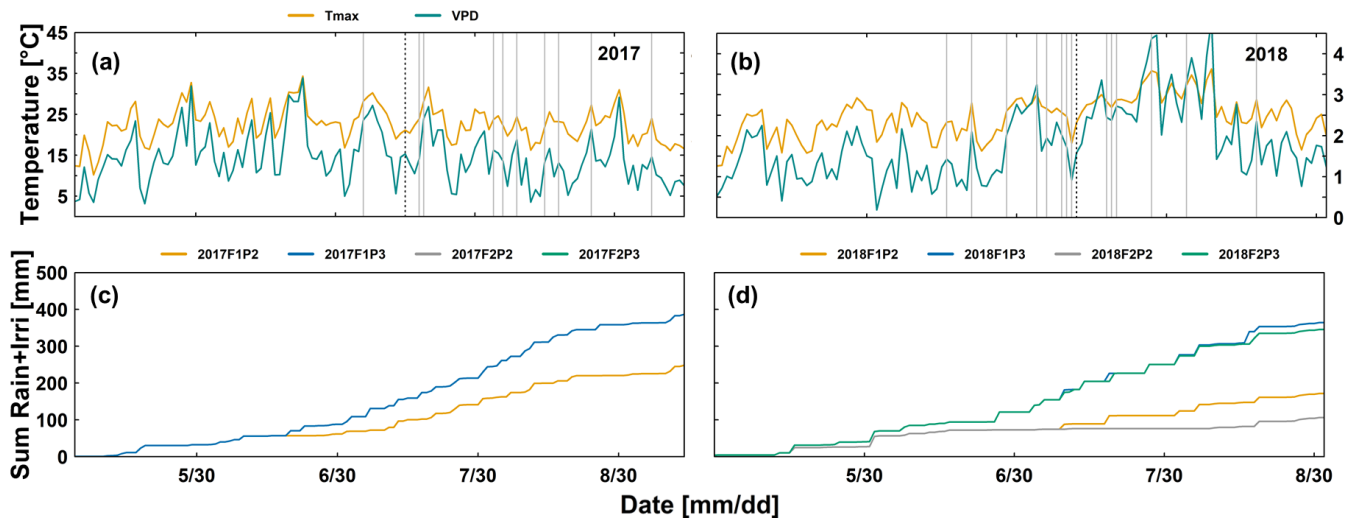
Figure 1: Daily maximum air temperature (Tmax) (°C), daily maximum air vapor pressure deficit (VPD) (kPa) in the two growing seasons (a) 2017 and (b) 2018 and cumulative (sum) of rainfall and irrigation from the rainfed (P2) and irrigated (P3) plots of the stony soil (F1) and silty soil (F2) in the two growing seasons (c) 2017 and (d) 2018. The black dashed vertical lines (a) and (b) indicate silking time. Grey vertical lines in (a) and (b) indicate the measured days for leaf gas exchange and leaf water potential. Two lines for 2017F2P2 and 2017F2P3 were overlapped by the lines from 2017F1P2 and 2017F1P3, respectively
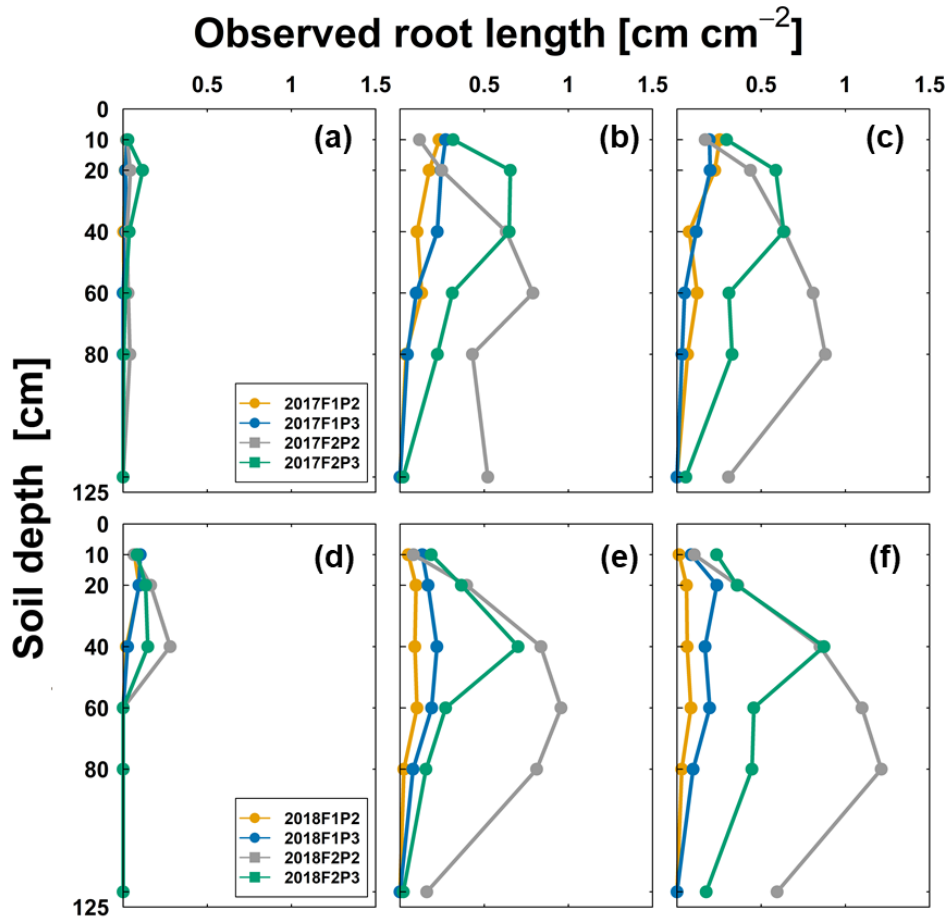
Figure 2: Observed root length from minirhizotubes (cm cm^{-2}) from 10, 20, 40, 60, 80, and 120 cm soil depth from the rainfed (P2) and irrigated (P3) plots of the stony soil (F1) and silty soil (F2) in the two growing seasons in 2017 (a - 8 June, b - at silking on 13 July, c - at harvest on 12 September) and in 2018 (d - 7 June, e - at one week after silking - 18 July, f - one week before harvest - 16 August).
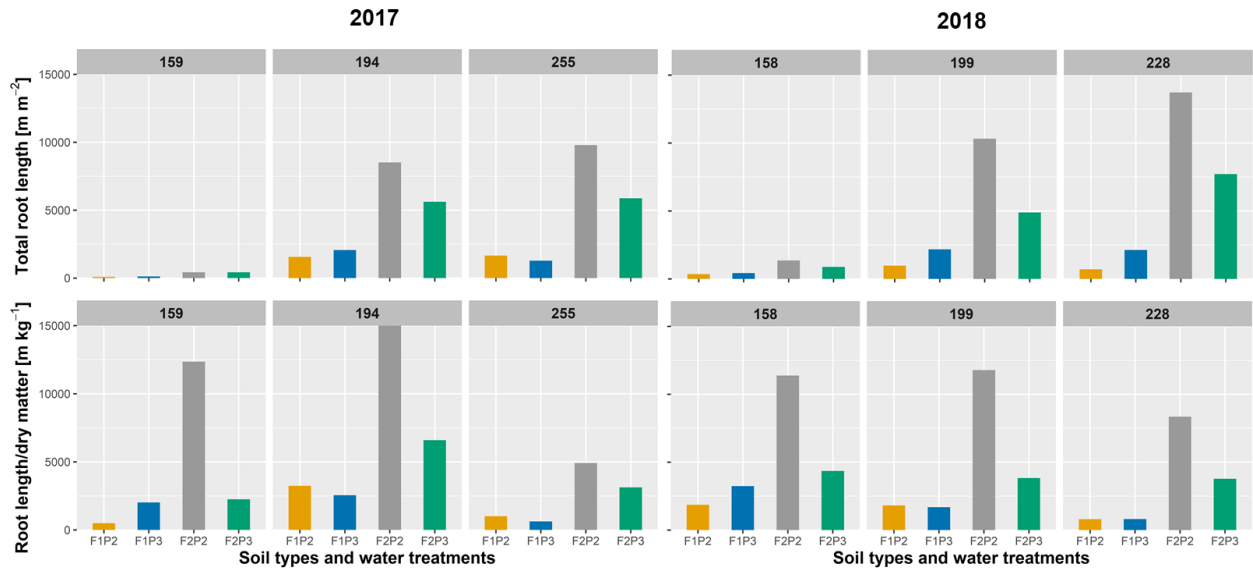
Figure 3: Observed root length from minirhizotubes (m m^{-2}) and ratio of root length per shoot dry matter (m kg^{-1}) from the rainfed (P2) and irrigated (P3) plots of the stony soil (F1) and silty soil (F2) in the two growing seasons (DOY 159, 194, and 255, left panel) in 2017 and in 2018 (DOY 158, 199, and 228, right panel) where on 8 June (DOY 159) at silking on 13 July (DOY194) 2017; and at harvest on 12 September (DOY 255) in 2017; 7 June (DOY 158), one week after silking on 18 July (DOY 199); and one week before harvest on 16 August (DOY 228) in 2018 (see also Figure 2).
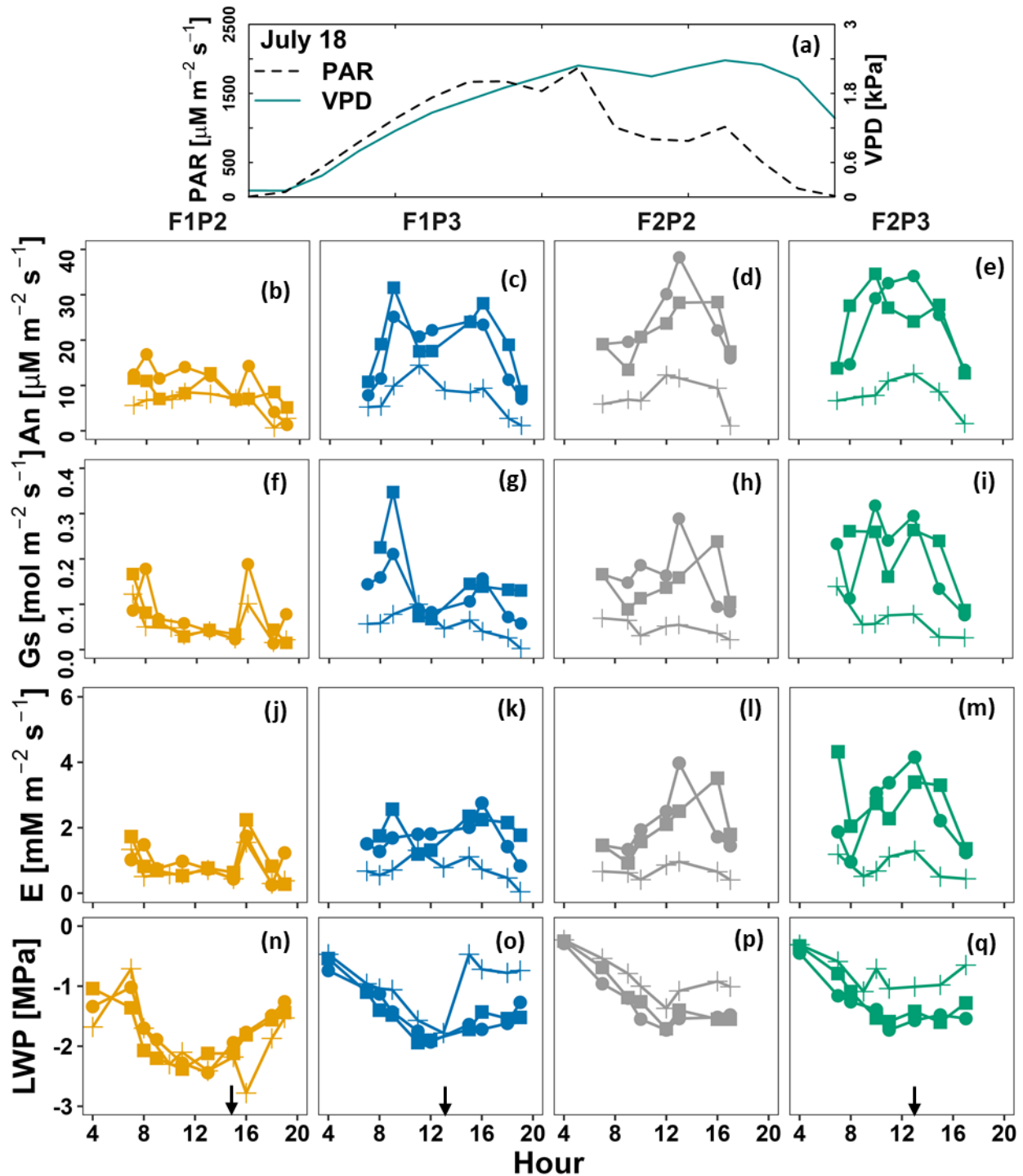
Figure 4. Diurnal course of (a) photosynthetically active radiation (PAR) and vapor pressure deficit (VPD), (b –e) leaf net photosynthesis (An), (f –i) leaf stomatal conductance (Gs), (j –m) leaf transpiration (E), and (n –q) leaf water potential (LWP) on 18 July in maize in 2018 before irrigation at the rainfed (P2) and irrigated (P3) plots of the stony soil (F1) and silty soil (F2). Measurement was carried out from shaded leaf (plus symbol with line) and two sunlit leaves (solid dot - lines and solid square - lines). Crop was irrigated at 1 PM, 1 PM, 4 PM for F1P3, F2P3, and F1P2, respectively (22.75 mm for each plot) (Supp. 2). Black arrows indicate time of irrigation.
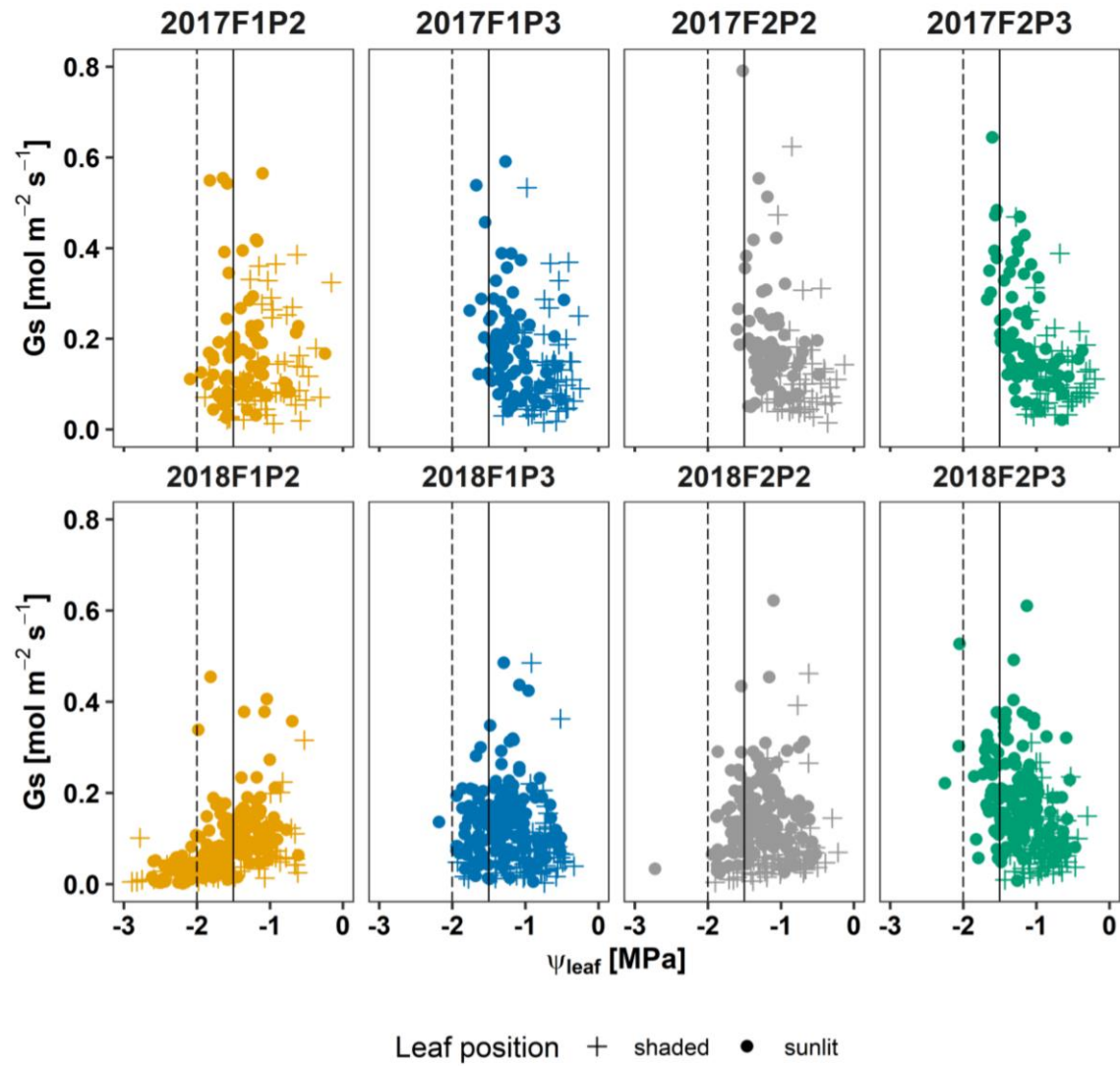
Figure 5: Seasonal stomatal conductance to water vapor (Gs) versus leaf water potential (ψ_{leaf}) in 2017 (top panel) and in 2018 (bottom panel) at the rainfed (P2) and irrigated (P3) plots of the stony soil (F1) and silty soil (F2). Vertically continuous and dashed lines indicated ψ_{leaf} at -1.5 and -2 MPa, respectively. Measurement was carried out from shaded leaf (plus symbol) and two sunlit leaves (solid dots)
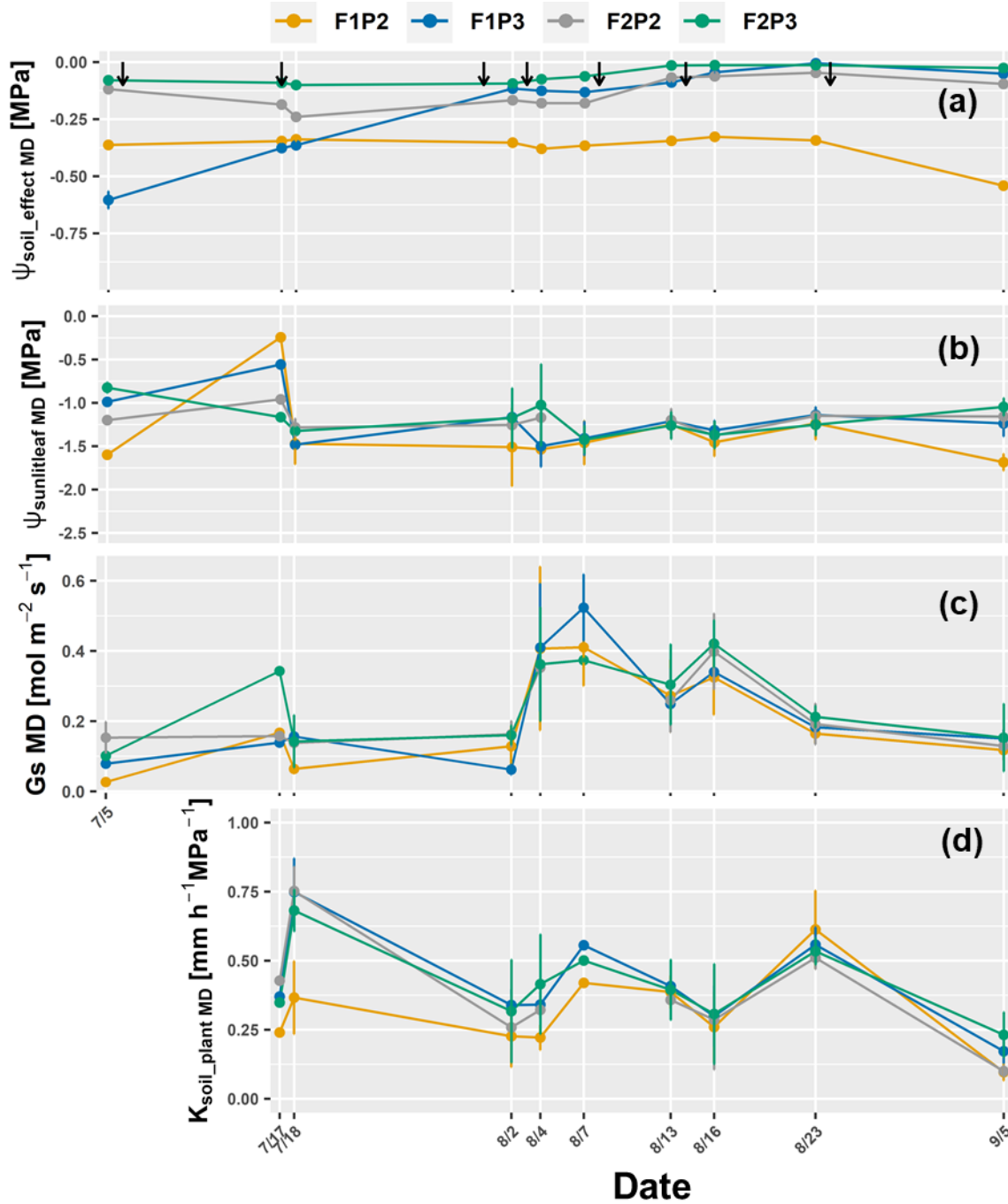
Figure 6: Dynamic of around midday (MD) of (a) the effective soil water potential ($\psi_{soil\_effec, MD}$) (b) sunlit leaf water potential ($\psi_{sunlitleaf MD}$), (c) stomatal conductance (Gs MD) and (d) whole soil-plant hydraulic conductance ($K_{soil\_plant MD}$) in the growing season 2017 from the rainfed (P2) and irrigated (P3) plots of the stony soil (F1) and silty soil (F2). Error bars indicate the standard deviation of the different values taken around midday (11 AM, 12AM, 1PM, and 2 PM) of different sunlit leaves. Whole soil-plant hydraulic conductance was shown from 17 July when sap flow was measured. The black arrows indicates the irrigation events for the irrigated treatments F1P3 and F2P3 in the showing period.
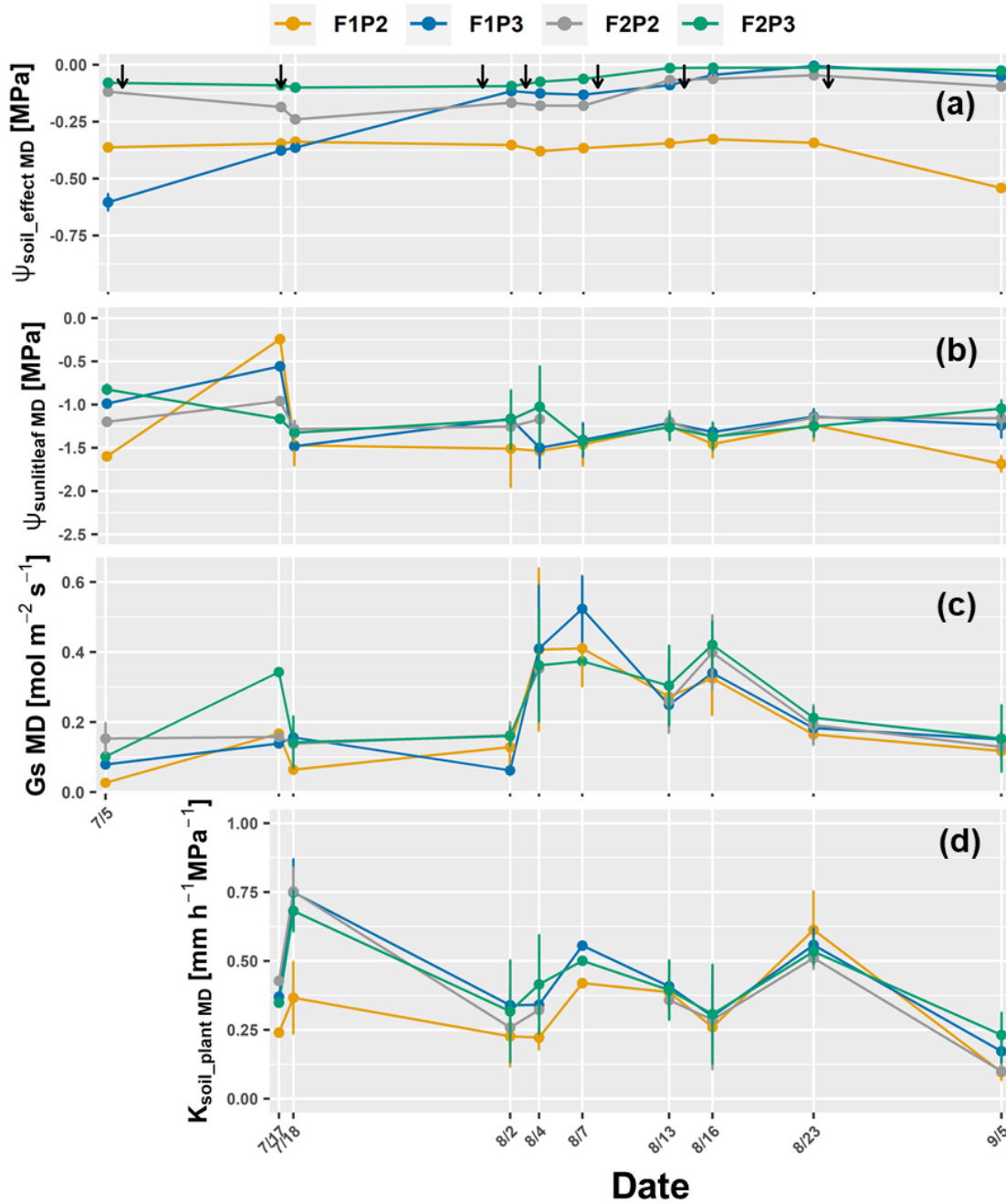
Figure 7: Dynamic of around midday (MD) of (a) the effective soil water potential ($\psi_{soil\_effec\ MD}$) (b) sunlit leaf water potential ($\psi_{sunlitleaf\ MD}$), (c) stomatal conductance (Gs MD) and (d) whole soil-plant hydraulic conductance ($K_{soil\_plant\ MD}$) in the growing season 2018 from the rainfed (P2) and irrigated (P3) plots of the stony soil (F1) and silty soil (F2). Error bars indicate the standard deviation of the different values taken around midday (11 AM, 12AM, 1PM, and 2 PM) Leaf water potential and stomatal conductance were 2 sunlit leaves and one shaded leaf at each measured hour. Whole soil-plant hydraulic conductance was shown from 3 July when sap flow was measured. The black arrows indicates the irrigation events for the irrigated treatments F1P3 and F2P3 while the orange arrow indicates the irrigation application for the rainfed plot at the stony soil (F1P2).
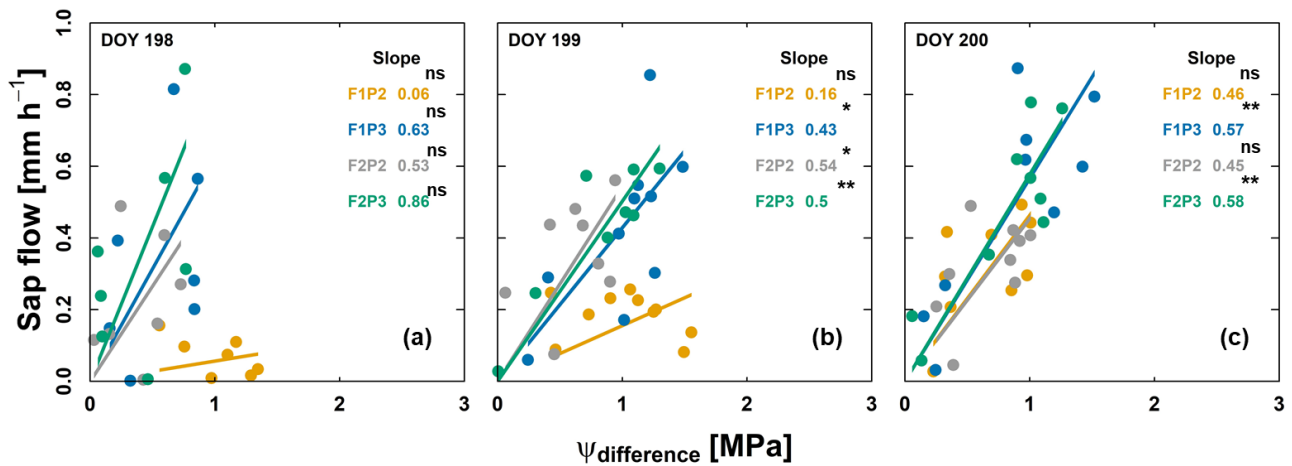
Figure 8: Relationship of sap flow and difference of effective soil water potential and sunlit leaf water potential ($\psi_{difference}$) from the rainfed (P2) and irrigated (P3) plots of the stony soil (F1) and silty soil (F2) on three consecutive measurement days from predawn in 2018 (a) 17 July - DOY 198, (b) 18 July - DOY 199 and (c) 19 July - DOY 200. Crop was irrigated on 18 July (DOY 199) at 1 PM, 1 PM, and 4 PM for F1P3, F2P3, and F1P2, respectively (22.75 mm for each plot). The unit of slope in the linear regression (or soil-plant hydraulic conductance) is mm h^{-1} MPa^{-1}. Regression was based on the DEMING approach. The asterisk which are next to the slopes indicate a significant correlation between two variables according to Pearson method (ns: non-significant; * $p < 0.05$; ** $p < 0.01$; *** $p < 0.001$).
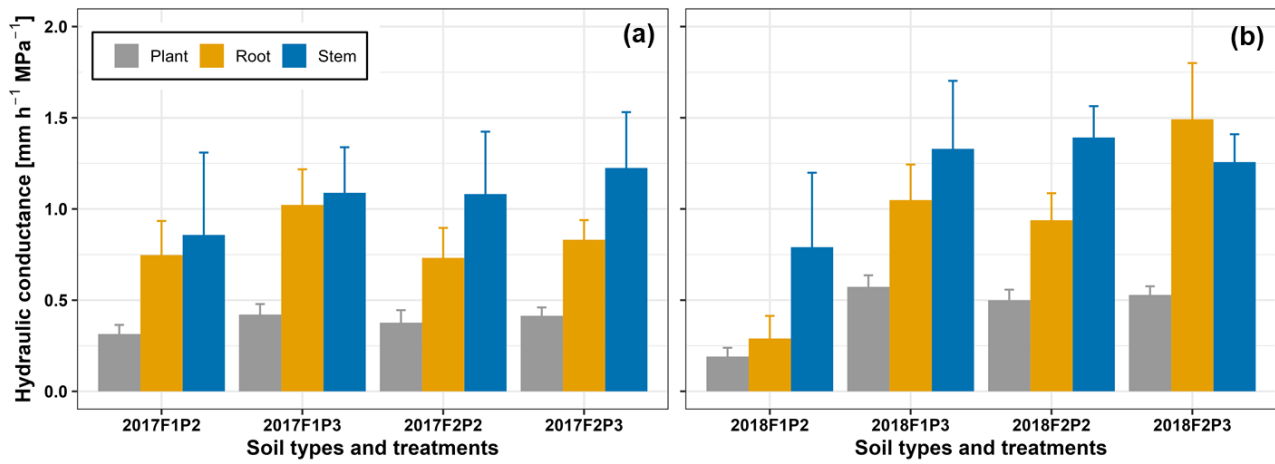
Figure 9: Comparison of different midday hydraulic components (mm h^{-1} MPa^{-1}): soil-plant (grey bars), soil-root (yellow bars), and stem (blue bars) from the rainfed (P2) and irrigated (P3) plots of the stony soil (F1) and silty soil (F2) in the two growing seasons (a) in 2017 and (b) in 2018. The error bars indicate the standard deviation from measurements around midday (11 AM, 12AM, 1PM, and 2 PM) in different measured days (in 2017 with n = 4 x 9 days, Supplementary material 10, 11, and Fig. 6 and in 2018 with n = 4 x 10 days, Supplementary material 10, 12, and Fig. 7).
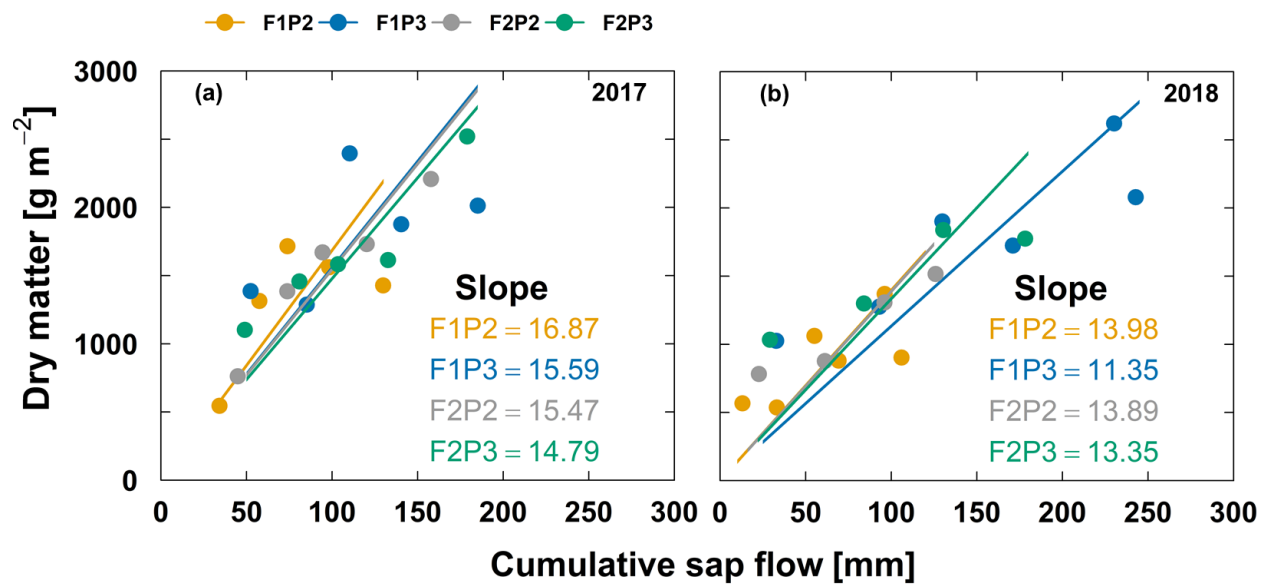
Figure 10: Relationship of aboveground dry matter and cumulative sap flow from the rainfed (P2) and irrigated (P3) plots of the stony soil (F1) and silty soil (F2) in the two growing seasons (a) 2017 and (b) 2018. The unit of slope linear relationship is g mm^{-1}. The less number of data points in (b) in 2018 from the F2P2 and F2P3 plots were due to the missing values of measured sap flow because of sensor disconnection. For aboveground dry matter, each point represents the average of two sampling replicates, except the harvest with 5 sampling replicates.